TU/e EINDHOVEN UNIVERSITY OF TECHNOLOGY

Molecular origin of physical ageing and rejuvenation in glassy polystyrene

Citation for published version (APA):
Grigoriadi, K. (2019). *Molecular origin of physical ageing and rejuvenation in glassy polystyrene*. [Phd Thesis 1 (Research TU/e / Graduation TU/e), Mechanical Engineering]. Technische Universiteit Eindhoven.

Document status and date:
Published: 05/06/2019

Document Version:
Publisher's PDF, also known as Version of Record (includes final page, issue and volume numbers)

Please check the document version of this publication:

• A submitted manuscript is the version of the article upon submission and before peer-review. There can be important differences between the submitted version and the official published version of record. People interested in the research are advised to contact the author for the final version of the publication, or visit the DOI to the publisher's website.
• The final author version and the galley proof are versions of the publication after peer review.
• The final published version features the final layout of the paper including the volume, issue and page numbers.

Link to publication

General rights
Copyright and moral rights for the publications made accessible in the public portal are retained by the authors and/or other copyright owners and it is a condition of accessing publications that users recognise and abide by the legal requirements associated with these rights.

• Users may download and print one copy of any publication from the public portal for the purpose of private study or research.
• You may not further distribute the material or use it for any profit-making activity or commercial gain
• You may freely distribute the URL identifying the publication in the public portal.

If the publication is distributed under the terms of Article 25fa of the Dutch Copyright Act, indicated by the "Taverne" license above, please follow below link for the End User Agreement:

www.tue.nl/taverne

Take down policy
If you believe that this document breaches copyright please contact us at:

openaccess@tue.nl

providing details and we will investigate your claim.

Download date: 17. Mar. 2025

Molecular Origin of Physical Ageing and Rejuvenation in Glassy Polystyrene

A catalogue record is available from the Eindhoven University of Technology Library. ISBN: 978-90-386-4777-7

This research forms part of the research programme of the Dutch Polymer Institute (DPI), Technology Area Performance polymers, DPI project #745.

This thesis was prepared with the LaTeX documentation system.
Cover conception: Kalouda Grigoriadi, Design: Anastasija Mass, Photography: George Vogiatzis. Models: Ahmad Amiri Rad, Caroline Balemans, Priscilla Brandão Silva, Robin Carpentier, Prakyat Hejmady, Tarek Kershah, Miroslava Lewinska, Stan Looijmans, Konstantinos Manikas, Jessica Pepe, Matilde Putti, Debarshi Saha, Wing-Hin Wong and Kalouda Grigoriadi.

© Copyright, 2019, Kalouda Grigoriadi. All rights reserved.

Molecular Origin of Physical Ageing and Rejuvenation in Glassy Polystyrene

PROEFSCHRIFT

ter verkrijging van de graad van doctor aan de Technische Universiteit Eindhoven, op gezag van de rector magnificus prof.dr.ir. F.P.T. Baaijens, voor een commissie aangewezen door het College voor Promoties, in het openbaar te verdedigen op woensdag 5 juni 2019 om 16:00 uur

door

Kalouda Grigoriadi

geboren te Corfu, Griekenland

Dit proefschrift is goedgekeurd door de promotoren en de samenstelling van de promotiecommissie is als volgt:

voorzitter:	prof.dr. L.P.H. de Goey
1^{e} promotor:	prof.dr.ir. P.D. Anderson
2^{e} promotor:	dr.sc.nat. M. Hütter
copromotor:	dr.ir. L.C.A van Breemen
leden:	prof.dr. K.U. Loos (RUG)
	prof.dr. R. Sijbesma
	prof.dr. G.B. McKenna (Texas Tech University)
adviseur:	dr.ir. P.A.M. Steeman (DSM)

Het onderzoek of ontwerp dat in dit proefschrift wordt beschreven is uitgevoerd in overeenstemming met de TU/e Gedragscode Wetenschapsbeoefening.

''If it disagrees with experiment, it's wrong. In that simple statement is the key to science. It doesn't make any difference how beautiful your guess is, it doesn't matter how smart you are who made the guess, or what his name is ... If it disagrees with experiment, it's wrong. That's all there is to it."

Richard Feynman

Contents

Acknowledgements

This work could not have been accomplished with the help of many wonderful people, whose names may not all be enumerated.

An exceptional gratitude to my thesis advisors, Markus Hütter and Lambèrt van Breemen and Patrick D. Anderson. I give them most of the credit for becoming the kind of scientist I am today.

A special mention to Michael Wübbenhorst, Tristan Putzeys and Alessia Gennaro. It was great to have the opportunity to work with you at the KU Leuven facilities.

Besides my advisors, I would like to thank the rest of my dissertation committee members Greg McKenna, Paul Steeman, Katja Loos and Rint Sijbesma for their crucial remarks that shaped my final dissertation.

I am also grateful to the following university staff: Lucien Cleven, Werner Neefs, Marc van Maris, Matilde Putti and Ellen van Heeswijk for their lab support and assistance.

To everyone at the Polymer Technology and MaTe Group.. it was great

to be my colleagues and friends.

Last but not least, I would like to express my deepest gratitude to my family, friends and my partner, Josè, for their support along the way.

Kalouda Grigoriadi

Eindhoven, June 2019

Summary

Physical ageing is present in all polymeric glasses, yet, its molecular origin is still under debate. Insight about the molecular origin of this process is of great scientific and technical importance. Physical ageing is generally known as the relaxation of an out-of-equilibrium state of a glass towards its equilibrium. This relaxation often has a catastrophic effect on the material properties. Macroscopically, a progressive increase of the yield stress is detected which can finally cause embrittlement. Heating a glass above its glass-transition temperature, T_g, is generally known to erase the thermomechanical history of the material, i.e. **thermal rejuvenation**. It is known that also the application of considerable stresses can erase the thermomechanical history of the glass, i.e. **mechanical rejuvenation**. Both thermal and mechanical rejuvenation lead to a decrease of the yield stress and enthalpy relaxation of the material. In the literature, most studies have focused on the effects of physical ageing and rejuvenation on the macroscopic properties of the material. Studies about the effect of these phenomena

on a molecular level are rather limited. This opens the route to the main goal of this thesis, which is:

To study the effect of thermal and mechanical rejuvenation and the successive ageing on the molecular dynamics.

This goal is achieved by studying polystyrene (PS), a material frequently used in both academia and industry. First, we focus on studying the effect of thermal rejuvenation and ageing on the molecular dynamics of a-PS, we continue with an investigation on the difference in molecular dynamics between thermal and mechanical rejuvenation, followed by molecular probing of the ageing effect after mechanical rejuvenation. Finally, the effect of molecular architecture (tacticity) on the physical ageing kinetics is examined. For the first three topics, broadband dielectric relaxation spectroscopy (BDRS) is employed, which is a technique that can follow the molecular dynamics over an extensive frequency range. Studies of polystyrene with BDRS are scarce because of the low capacitance of the material. To tackle this problem, we carefully chose the equipment and the preparation protocol for the samples.

First, we studied the effect of physical ageing on the molecular dynamics of atactic polystyrene upon thermal rejuvenation, short-term (six weeks), and long-term (one year) ageing under ambient conditions. In addition,

attenuated total reflection Fourier transform infrared spectroscopy (ATR-FTIR) measurements were performed to connect the molecular dynamics with the changes of the molecular structure (phenyl-ring *trans*-population) during ageing. Using these techniques, the homogenization of the system together with the energetically favorable increase of the phenyl-ring *trans*-population is observed. Interestingly, an increase of localized low-amplitude motion of the polymeric chains is also noticed.

Second, using the same techniques, we investigate the molecular mechanisms responsible for mechanical rejuvenation by cold rolling, unravelling striking differences in the molecular dynamics of the thermal and mechanical rejuvenation. Upon cold rolling the system is enriched on the molecular scale with three new relaxation processes. At the same time, through ATR-FTIR, an increase of the phenyl-ring *trans*-conformers is observed, which together with polarized-light microscopy reveals orientation in the system.

Third, ageing of the cold-rolled atactic polystyrene and the corresponding molecular mechanisms were examined, showing that two relaxation processes are suppressed, and there are losses in molecular mobility (BDRS) and chain orientation (ATR-FTIR).

For the fourth topic, we applied flash differential scanning calorimetry (flash-DSC), the only technique that can cool and heat the material rapidly, hence, probe the still unexplored effect of molecular architecture on

physical ageing kinetics of atactic, syndiotactic and isotactic PS, starting from a fully amorphous rejuvenated state. Here, it is proven that the molecular architecture plays a significant role on the kinetics of physical ageing: syndiotactic PS ages slowest, the atactic faster, and the isotactic PS shows the fastest ageing kinetics.

In summary, the conclusions of the thesis on the molecular origins of physical ageing, thermal and mechanical rejuvenation are the following:

- Thermal and mechanical rejuvenation are two phenomena with significantly different molecular dynamics; mechanical rejuvenation shows three new relaxation processes, fast molecular dynamics and chain orientation, while thermal rejuvenation is characterized by main-chain segmental relaxation and a process connected to low-amplitude chain movements. Finally, the molecular structure is in a high-energy state (low *trans-trans* population).

- Short-term physical ageing after mechanical rejuvenation shows a decrease of molecular mobility, increased homogeneity (hindering of two processes) in the system and a decrease of chain orientation; in contrast, short-term physical ageing after thermal rejuvenation is governed by an increased molecular mobility and low-energy molecular states (increased *trans-trans* population).

- Tacticity does affect physical ageing; syndiotactic and isotactic sequences lead to the two extremes, slow and fast ageing kinetics, respectively, while atactic sequences show ageing kinetics between these two extremes.

Chapter 1

Introduction

1.1 Background

The state of a glass is certainly one of the most intriguing topics in condensed matter science. The frequent use of polymeric glasses in high-level applications, such as polymer optics[1], industrial gas separation membranes[2,3], hyperbaric windows[2], drug delivery systems[4], makes the mastery of molecular mechanisms responsible for their macroscopic behavior of utmost importance.

Not very long ago, in the late 1970s, the Food and Drug Administration

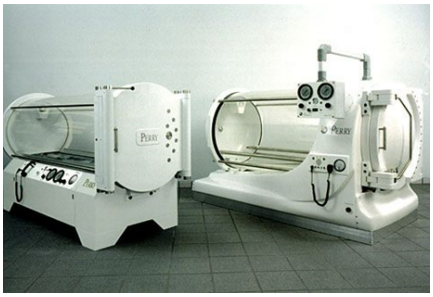

(a)

(b)

Figure 1.1: (a) Hyperbaric chamber[5] and (b) polymer optics[6].

(FDA), approved the use of amorphous poly(ethylene terephthalate) (PET) for use as bottles that contain water[7]. In a short time after the launch of the bottles to the market, a puzzling phenomenon was observed: Shortly after storing the PET bottles in warehouses at elevated temperatures, it was observed that the macroscopic properties of the material were altered. Namely, the material became brittle. Soon after, this phenomenon was named physical ageing[8]. It is the evolution of the out-of equilibrium glass towards equilibrium. Except of embrittlement, changes occur also for other properties, such as water permeation[9], oxygen diffusion[10] and specific enthalpy[11]. The molecular mechanisms of how these changes occur is still an enigma for the scientific community. Physical ageing can be erased by increasing the temperature of the polymeric glass above its glass-transition temperature, T_g, which is therefore called thermal rejuvenation[12]. Additionally,

it is commonly recognized that deformation can also lead to the erasure of (some aspects of) physical ageing, a phenomenon known as mechanical rejuvenation[12]. Macroscopically, thermally or mechanically rejuvenated glasses have similar properties, e.g., a decreased yield stress[13]. However, from a microscopic point of view, they might be significantly different due to, for example, the anisotropy introduced from the deformation process. Likewise, the physical ageing after thermal or mechanical rejuvenation is considered to be of the same nature macroscopically, but the molecular origins of the two types of ageing seem to be of a different kind[14].

Despite the ongoing research on the effect of ageing on the mechanical, thermal and dynamical properties, there is limited knowledge about the corresponding microscopic aspects. Therefore, a microscopic investigation on the molecular origins of physical ageing and rejuvenation is of utmost relevance.

1.2 Current state of the art

In the early years of research on the physical ageing, it was appreciated that physical ageing results in the increase of the yield stress[13,15] and enthalpy overshoot of the material[16]. Furthermore, heating the material above its glass-transition temperature or imposing a large deformation after physi-

cal ageing is considered to cause rejuvenation through generation of free volume[17], which also can be seen by a decreased enthalpy overshoot[16].

However, later research on these properties brought to light new findings. Various properties of interest of polymeric glasses in ageing and rejuvenation, such as macroscopic (e.g. yielding) and microscopic (e.g. segmental relaxation times) properties have been investigated in numerous studies, as discussed in the following.

Van Melick et al.[13] in their study on the yielding kinetics and creep compliance of atactic polystyrene (a-PS) found that the ageing rate for cold-rolled samples was considerably different than for thermally rejuvenated ones. Similar results have been obtained by Nazai et al.[18] on the compressive yield stress of thermally and mechanically rejuvenated PMMA.

Other groups obtained information for changes in other properties, such as enthalpy relaxation. Here, no correlation with yielding kinetics data could be made, while it is generally acknowledged that the enthalpy relaxation increases with ageing[15,19,20]. Furthermore there is a significant difference between the deformed and undeformed enthalpy measurements: the deformed specimens show, except of the enthalpy overshoot in the T_g-region, an endothermic peak around 30 °C below T_g, which is attributed to the stored internal energy of the system due to deformation[21,22]. While enthalpy measurements give some information about the differences bet-

ween deformed and undeformed measurements, structural information is still lacking.

Although there was some evidence that ageing after mechanical rejuvenation has faster kinetics than after thermal rejuvenation, explained by a higher molecular mobility, evidence from measuring other properties, such as density, was rather controversial: Density measurements of PS[13], PC[23], ABS[23] and PVC[23] show, that the density of the material increased with mechanical deformation. How that could connect with the probably higher molecular mobility of the mechanically rejuvenated specimens remains unclear to this point.

In order to get more information about the free-volume changes of glassy polymers upon rejuvenation and ageing, various groups[24,25] applied positron annihilation lifetime spectroscopy (PALS). It was observed that the free-volume holes concentration was decreased with ageing after thermal rejuvenation. Differently, ageing after mechanical deformation showed a stable concentration of free-volume holes but also a reduction of their size, implying a different microstructure.

Direct dielectric spectroscopy experiments focus on the segmental mobility during deformation, which proved to be increased[26–28]. Molecular modeling supports the idea that the increased molecular mobility observed for the deformed studies is due to the exploration of different regions in the

energy landscape as compared to thermal rejuvenation[29,30].

Recently, researchers have studied with Fourier transform infrared spectroscopy (FTIR) various glassy polymers and a common trend has been revealed: with the course of ageing, the conformations of the polymers rearrange into the energetically more stable states. For example, for polycarbonate (PC) the *trans-cis* conformers rearrange into the *trans-trans* counterparts[31]. Unfortunately, there is no information available in the literature for mechanical rejuvenation and subsequent ageing.

Many microscopic studies have revealed that plastic deformation creates a heterogeneous structure[14], transmission electron microscopy (TEM) and small-angle X-ray scattering (SAXS)[32] have shown the formation of fibrilar material which heals with ageing[33].

In summary, the information in literature cannot give an indisputable explanation for the molecular mechanism behind the ageing after thermal and mechanical rejuvenation.

1.3 Scope of the thesis

The scope of this thesis is to study the molecular origins of physical ageing, the molecular differences between the thermal and mechanical rejuvenation, and the effect of tacticity on the ageing kinetics of amorphous PS. To that

end, we use broadband dielectric relaxation spectroscopy (BDRS) which is one of the techniques that can follow the molecular dynamics in a broad frequency and time range, which is essential for the investigation of physical ageing and rejuvenation on small scales. Furthermore, we choose to study polystyrene (PS), a material known for its fast ageing kinetics and which has been studied extensively by simulations. However, choosing PS comes

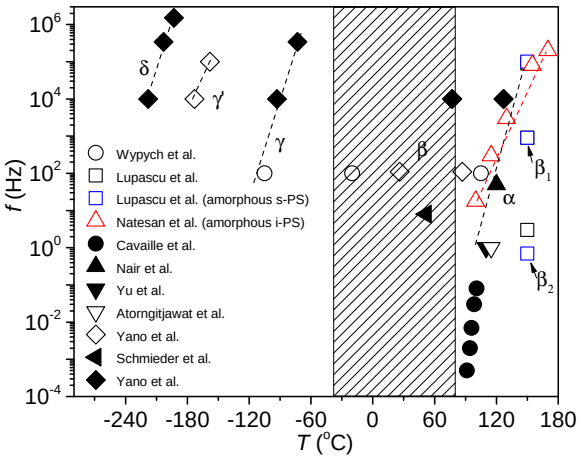

Figure 1.2: Literature compilation of dielectric spectroscopy (empty symbols) and dynamic mechanical analysis (filled symbols) data for a-PS (black symbols), amorphous s-PS (blue symbols) and amorphous i-PS (red symbols). The data are taken from the work of: Wypych et al.[34], Lupaşcu et al.[35], Natesan et al.[36], Cavaille et al.[37], Nair et al.[38], Yu et al.[39], Atorngitjawat et al.[40], Yano et al.[41] and Schmieder et al.[42].

with a challenge since it is a material having a weak relaxation strength, which makes it difficult to be studied by BDRS; we overcome this challenge by choosing specific equipment and careful sample preparation. Moreover, the relaxation processes of amorphous PS, specifically for the β-relaxation, are controversial, as can be seen in the shaded region in Figure 1.2. To study the effect of ageing on enthalpy kinetics of amorphous PS we use flash differential scanning calorimetry (flash-DSC) with high heating and cooling rates, to ensure the preparation of amorphous samples and well-defined ageing studies.

The thesis starts with **Chapter 2**, where we investigate the molecular dynamics of a-PS upon thermal rejuvenation and physical ageing at ambient conditions for short-term (six weeks) and long-term ageing times (one year). BDRS was used to probe the changes of the molecular dynamics, while complementary FTIR measurements connect the changes in molecular dynamics with changes in molecular structure.

Chapter 3 provides a BDRS study on the differences between mechanically, by cold rolling and quenching, and thermally rejuvenated a-PS. Complementary FTIR and polarized-light microscopy measurements connect the local and cooperative dynamics with molecular structure changes and nanoscale structural changes, respectively.

The thesis continues with **Chapter 4**, in which the cold-rolled a-PS is

subjected to ageing at 50 °C under nitrogen atmosphere, and its molecular dynamics are characterized by BDRS. FTIR measurements complement the molecular picture.

Chapter 5 presents a detailed investigation on the effect of tacticity on the physical ageing kinetics of amorphous atactic, syndiotactic and isotactic PS. FDSC was used for this study.

Finally this dissertation closes with **Chapter 6**. Here a discussion of the results is summarized and some recommendations for further research are given.

Chapter 2

Effect of low-temperature physical ageing on the dynamic transitions of atactic polystyrene in the glassy state

Abstract: The local and cooperative dynamics of atactic PS (a-PS) were studied by broadband dielectric relaxation spectroscopy (BDRS) and

This chapter is largely reproduced from: K. Grigoriadi, T. Putzeys, M. Wübbenhorst, L.C.A van Breemen, P.D. Anderson, M. Hütter. "Effect of low-temperature physical ageing on the dynamic transitions of atactic polystyrene in the glassy state". *J. Polym. Sci. B Pol. Phys.* Submitted.

attenuated total reflectance Fourier transform infrared spectroscopy (ATR-FTIR). The a-PS has been subjected to thermal rejuvenation and subsequent quenching, short-term ageing (six weeks) and long-term ageing (one year) at ambient conditions. Where for the rejuvenated sample only an α- and a γ-relaxation is observed, short-term ageing results in an additional β^*-relaxation that merges with the α-relaxation at longer ageing times. The γ-relaxation is increasing in intensity and activation energy during ageing. The α-process shows no spectral changes and shift in the relaxation time upon ageing. This may be attributed to a possible erasure of history of the material during the temperature-sweep mode measurement. Fourier transform infrared spectroscopy (FTIR) results suggest that the energetically favorable *trans-trans (tt)* conformers are increased in population with ageing.

2.1 Introduction

Below the glass-transition temperature T_g, glasses are known to be in a non-equilibrium state and their relaxation towards equilibrium is called physical ageing[8]. Physical ageing causes a slow alteration of the physical structure of the material. This alteration often has a detrimental effect on the material properties. Macroscopically, a gradual increase of the yield stress of the material is observed, which causes embrittlement[13], resulting in a gradual loss of the design function and ultimate failure. These macroscopic changes make physical ageing of enormous importance, both on a technical and research level.

Numerous studies have been done to examine the effect of physical ageing on the macroscopic mechanical behavior of glassy polymers[43–48] and similarly for the enthalpy changes upon ageing[20,48–53]. Most of the studies are trying to explain their results based on the free-volume theory[8], in which the changes of the properties of the material are interpreted solely by the changes in free volume[24,54–57]. Other studies try to explain their results from the stand-point of segmental/chain mobility[58,59]. However, the link between the molecular structure and intrinsic properties is still lacking.

Since many physical properties of glassy polymers are affected by physical ageing, a large variety of techniques can be used to study them; ho-

wever, only a few studies can follow the dynamics over a broad frequency range, which would be necessary for studying the effects of physical ageing on small scales. One of these methods is broadband dielectric relaxation spectroscopy (BDRS), which covers more than ten decades in time and frequency. Most of the research studies involve measurements of relaxations close to the glass-transition[60], and only a few are dedicated to measure the effect of ageing on the secondary relaxations below T_g[61]. So far, dielectric relaxation spectroscopy has very limited use in studying ageing of atactic polystyrene (a-PS)[34], because the measurements are known to be difficult due to the weak relaxation strength of the material.

In this work, we study rejuvenated and fast cooled (cooling rate $\approx$ 230 K/min) a-PS using dielectric and ATR-FTIR spectroscopy, and compare the results with short- and long-term aged a-PS samples stored at room temperature. Complementary BDRS and ATR-FTIR studies allow us to relate changes in the molecular dynamics with changes in molecular conformations during physical ageing.

2.2 Experimental section

2.2.1 Materials

Atactic PS with the commercial name N5000 was kindly supplied in pellet form by Shell. The molecular weight (M_w = 320.700 g/mol) and polydispersity index (PDI = 2.22) were determined by High-Performance Liquid Chromatography (HPLC) using a Shimadzu HPLC instrument (Prominence -I, LC 2030C 3D).

2.2.2 Sample preparation

Films of 0.13 mm thickness were prepared by compression molding under vacuum at a temperature of 185 °C. First, the pellets were heated for five minutes and then compressed in three steps of increasing pressure from ≈ 23 MPa up to ≈ 70 MPa. Afterwards, the mold was cooled down to room temperature between two cold metal plates at a pressure of approximately 23 MPa.

The obtained films were recompressed between two Kapton foils under vacuum at 185 °C at ≈ 70 MPa for ten minutes to eliminate surface roughness. Afterwards the mold was cooled down at ambient conditions.

2.2.3 Treatments

The samples were prepared for the dielectric and ATR-FTIR spectroscopy measurements as follows. The PS films were thermally rejuvenated by heating them to 140 °C for half an hour and subsequently quenching them in liquid nitrogen (cooling rate ≈ 230 K/min). The samples were flushed with nitrogen gas to avoid water condensation on their surface. Afterwards, the films were aged for six weeks (called "short-term aged" hereafter) and one year (called "long-term aged" hereafter) respectively, at room temperature and Relative Humidity (RH) ≈ 30%.

2.2.4 Broadband dielectric relaxation spectroscopy (BDRS)

Dielectric measurements in a temperature/frequency sweep-mode, from 10^{-1} Hz to 10^{6} Hz, and from -120 °C to 145 °C in steps of 5 K, leading to an effective heating rate of around 0.5 K/min. A high-accuracy dielectric analyzer (ALPHA analyzer, Novocontrol Technologies) in combination with a Novocontrol Quatro temperature system maintaining excellent control of the sample temperature ($\leq$ 0.05 K) was used. The samples (40 mm in diameter and a thickness of 0.13 mm) were placed between polished stainless steel electrodes.

To determine the relaxation time $\tau(T)$ and other relaxation parameters, the dielectric loss spectra $\varepsilon''(\omega)$, obtained for different temperatures

(Figure 2.1), were fitted to the imaginary part of the Havriliak-Negami (HN) relaxation function[62],

$$\varepsilon'' = -\mathrm{Im}\left\{\frac{\Delta\varepsilon}{(1+(i\omega\tau)^a)^b}\right\} + \frac{\sigma}{\varepsilon_\nu\omega}, \tag{2.1}$$

where $\Delta\varepsilon$ denotes the relaxation strength, while the two "shape parameters" a and b relate to the logarithmic slope of the low-frequency loss tail (a) and the high-frequency loss tail (ab). The second term of the right-hand side of Equation 2.1 accounts for the Ohmic conduction, where σ corre-

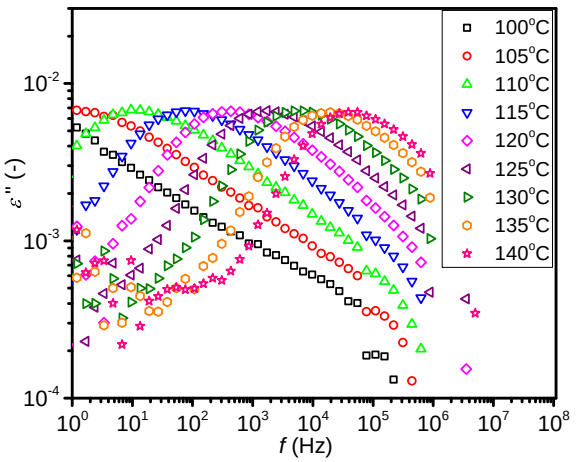

Figure 2.1: Dielectric loss spectra $\varepsilon''(f,T)$ for various temperatures showing the dynamic glass-transition α-process.

sponds to the conductivity, ε_ν to the vacuum permittivity and $\omega = 2\pi f$ to the angular frequency. An extensive description of the analysis procedure for dielectric features can be found in the studies of Wübbenhorst et al.[63] and Van Turnhout et al.[64].

2.2.5 Attenuated total reflectance Fourier transform infrared spectroscopy (ATR-FTIR)

ATR-FTIR spectroscopy in reflection mode (PERKIN ELMER Spectrum two spectrometer) was carried out on the PS films in the range from 400-4000 cm^{-1} at a resolution of 4 cm^{-1}, with a total of 50 scans. Two such measurements were performed on each sample. A normalization protocol was applied to erase the effect of sample thickness in the absorbance spectrum. FTIR spectra contain absorption bands that are specific to both *trans-trans* and *trans-gauche* conformations[65], while other bands (ring modes) show no conformation sensitivity and thus provide an internal reference. Specifically, the original spectra of the conformationally sensitive 538 cm^{-1} peak were normalized with the 1451 cm^{-1} peak that does not represent conformational changes and thus is used as an internal reference.

2.3 Results

2.3.1 Dielectric relaxations

The molecular dynamics of thermally rejuvenated, short- and long-term aged (ambient conditions) a-PS were studied by BDRS. The relaxation behavior of the a-PS is given in Figures 2.2, 2.3 and 2.4. The representation of tanδ ($= \varepsilon''/\varepsilon'$) is chosen, since tanδ eliminates uncertainties with samples thickness, while the peak shape is preserved due to the low relaxation strength of all processes[63]. In Figure 2.2, the tanδ as a function of temperature are represented for the thermally rejuvenated sample, a short-term aged (at 20 °C) sample and a long-term aged (at 20 °C) sample, as recorded at a frequency of 100 Hz. In Figure 2.3, the tanδ as a function of frequency in the temperature-range where a specific process is visible are shown for the thermally rejuvenated sample, the short-term aged and the long-term aged samples. The resulting spectra of thermally rejuvenated a-PS samples reveal the main α-relaxation process, also found in literature[8,45], whereas no second process, β, appears in the whole frequency range (Figures 2.2-2.3b). The γ-process appears at -110 °C (Figure 2.2). In contrast, both aged samples show an additional β^*-process just below the α-relaxation and well above the γ-relaxation range. For longer ageing times, this β^*-process becomes a shoulder of the main α-relaxation process. At the measured

frequencies and temperatures, not the whole peak but only the tail of the β^*-process is shown in Figure 2.3.

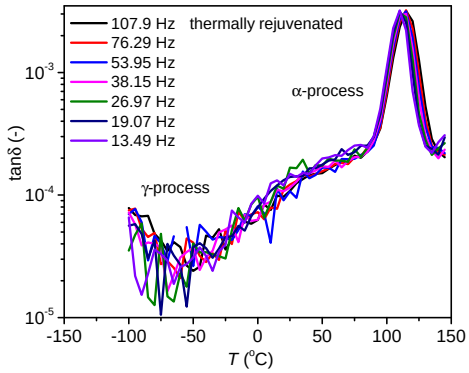

(a)

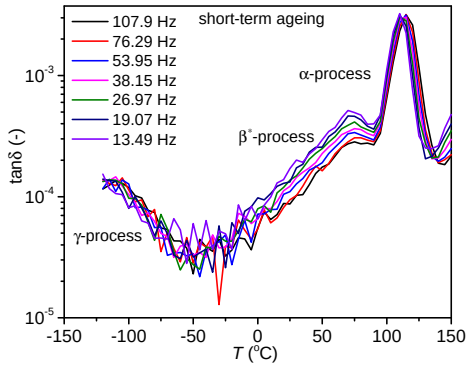

(b)

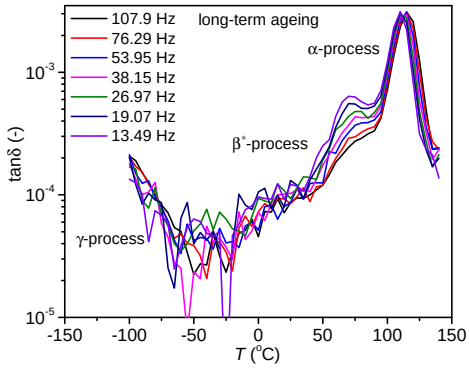

(c)

Figure 2.2: Snapshot of dielectric spectra of loss tangent tanδ versus temperature T as measured at frequencies of about 14 Hz, 19 Hz, 27 Hz, 38 Hz, 54 Hz, 76 Hz and 108 Hz for (a) the thermally rejuvenated a-PS, (b) short-term aged and (c) long-term aged sample. The data were obtained by heating the sample from -120 °C to 145 °C at a heating rate of about 0.5 K/min.

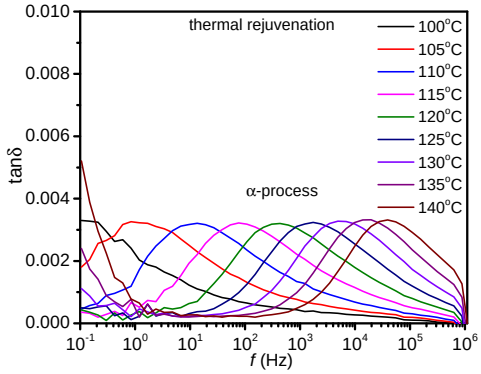
thermal rejuvenation
α-process
100°C
105°C
110°C
115°C
120°C
125°C
130°C
135°C
140°C
tanδ
f (Hz)

(a)

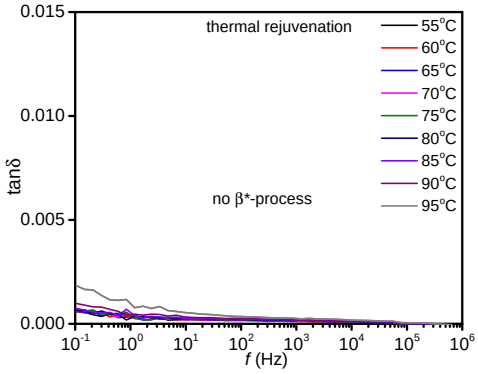
thermal rejuvenation
no β*-process
55°C
60°C
65°C
70°C
75°C
80°C
85°C
90°C
95°C
tanδ
f (Hz)

(b)

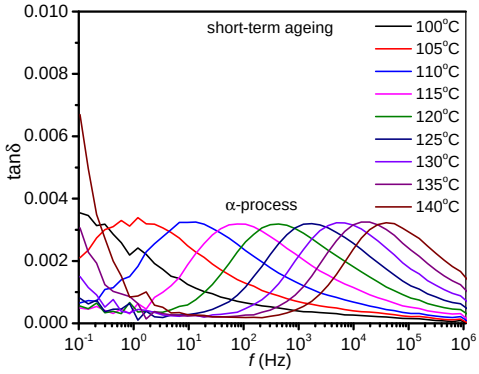
short-term ageing
α-process
100°C
105°C
110°C
115°C
120°C
125°C
130°C
135°C
140°C
tanδ
f (Hz)

(c)

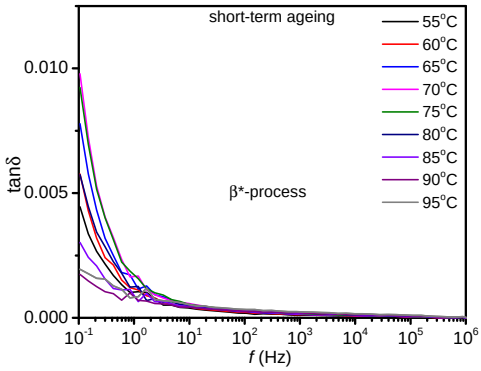
short-term ageing
β*-process
55°C
60°C
65°C
70°C
75°C
80°C
85°C
90°C
95°C
tanδ
f (Hz)

(d)

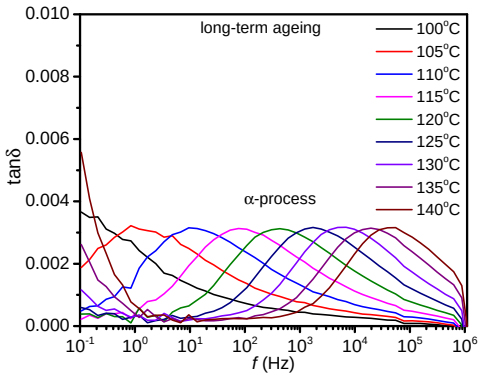
long-term ageing
α-process
100°C
105°C
110°C
115°C
120°C
125°C
130°C
135°C
140°C
tanδ
0.010
0.008
0.006
0.004
0.002
0.000
10-1
100
101
102
103
104
105
106
f (Hz)

(e)

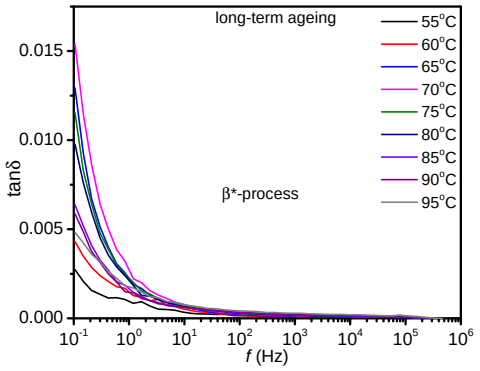

(f)

Figure 2.3: Dielectric loss tangent $\tan\delta(f, T)$ for various temperatures, showing the dynamic glass-transition temperature (a) and the β^*-process (b) for the rejuvenated, dynamic glass-transition temperature (c) and the β^*-process (d) for the short-term aged, and dynamic glass-transition temperature (e) and the β^*-process (f) for the long-term aged a-PS. The data were obtained by heating the sample from -120 °C to 145 °C at a heating rate of about 0.5 K/min.

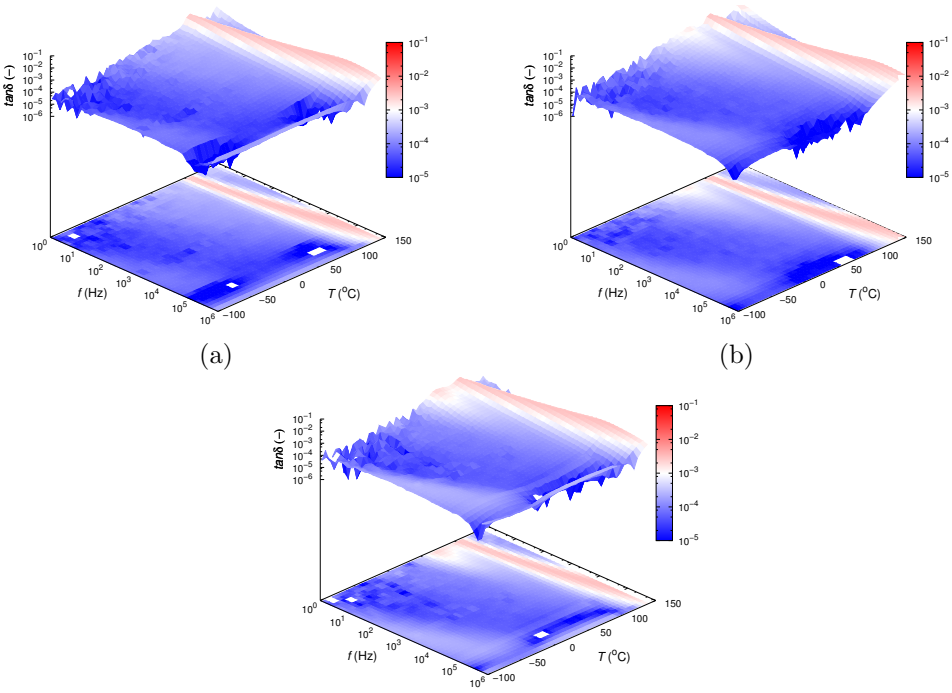

Figure 2.4: Three-dimensional representation of the dielectric loss tangent $\tan\delta(f, T)$ for (a) the thermally rejuvenated, (b) short-term aged, and (c) long-term aged a-PS.

The dielectric input was examined by fitting isothermal spectra $\varepsilon''(\omega)$ to Equation 2.1, to calculate the complete relaxation and thermal activation parameters. The relaxation-time data are shown in the Arrhenius diagram (Figure 2.5). The α-process distinguished by its representative curvature in the temperature dependence of the relaxation time, $\tau(T)$, was fitted to

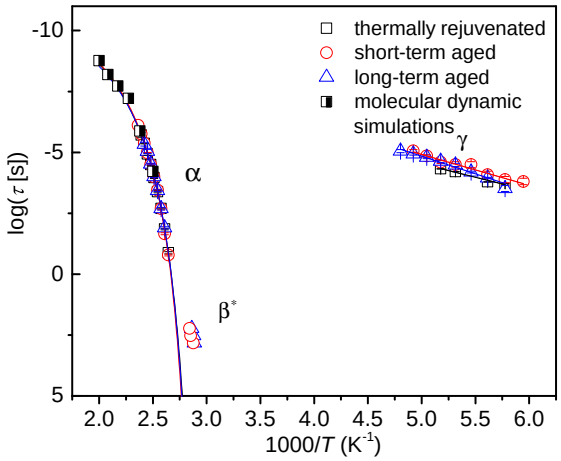

Figure 2.5: Activation diagram showing the peak relaxation times τ_α and τ_γ for three different treatments of a-PS: thermal rejuvenation (black squares), short-term ageing (red squares) and long-term ageing (blue squares). Molecular dynamics simulations of a-PS (black and white squares) (courtesy of G. G. Vogiatzis). Lines: fit with Equation 2.2 and Equation 2.3, respectively. Note: the β^*-relaxation data points are obtained from the respective peak-positions in the $\varepsilon''(T)$-graphs (Figures 2.2b and 2.2c), and using $\tau = 1/(2\pi f)$.

Table 2.1: Activation parameters and their standard deviation for the α- and γ-processes found in a-PS for the different treatments.

	α-process		
treatment	$\log(\tau_\infty[s])$	E_V(kJ/mol)	T_V(K)
thermally rejuvenated	-11.86±0.04	10.7±0.2	327.270±0.008
short-term aged	-11.78±0.06	10.1±0.3	330.220±0.012
long-term aged	-11.55±0.05	9.8±0.3	330.000±0.001
	γ-process		
treatment	$\log(\tau_\infty[s])$	E_A(kJ/mol)	
thermally rejuvenated	-9.99±1.75	20.9±8.7	
short-term aged	-11.10±0.10	23.6±0.5	
long-term aged	-12.51±0.06	29.3±0.3	

the Vogel-Fulcher-Tamman (VFT) law[64],

$$\tau = \tau_\infty \exp\left(\frac{E_V}{R(T - T_V)}\right), \tag{2.2}$$

where E_V and T_V are the Vogel activation energy and the Vogel temperature, respectively. The additional two parameters R and τ_∞ are the universal gas constant and the ultimate relaxation time, respectively. Contrary, the γ-relaxation data follow the Arrhenius equation, Equation 2.3, suggestive for "simple" thermally activated response,

$$\tau = \tau_\infty \exp\left(\frac{E_A}{RT}\right), \tag{2.3}$$

with activation energy E_A and ultimate relaxation time $\log\tau_\infty$. All fit

parameters for the three relaxations are noted in Table 2.1. The dielectric activation map for the α- and γ-relaxations for all the reference and aged samples is shown in Figure 2.4. Evidently, the effect of ageing is different for each molecular relaxation in a-PS. The width as well as the relaxation times of the α-relaxation do not change significantly with ageing (Figures 2.2, 2.3a, 2.3c, 2.3e and Table 2.1), while the Vogel activation energy of this process is in agreement with other studies[66,67].The β*-process did not appear in a rejuvenated sample (Figures 2.2a, 2.3b and 2.4a), though, for six weeks of ageing the peak of this process appeared at 73 °C (100 Hz). After one year of ageing at room temperature, the β*-process peak increased in intensity (Figure 2.2c) and became a shoulder of the α-process (Figure 2.4). Moreover, the β*-process for both short- and long-term aged samples shows a peculiar behavior: the losses increase with increasing temperature up to 70 °C (Figures 2.3d-2.3f). Increasing the temperature from 70 °C to 90 °C, the losses decrease. Unfortunately, only the tail of the β*-process appears in a short frequency range (10^{-1}-10^{0} Hz) only (Figures 2.3d-2.3f), which makes the determination of the relaxation time and activation energy of this relaxation process unreliable (see Appendix). The γ-process had a profound increase in intensity of tanδ and activation energy with ageing (Figures 2.2 and 2.4, Table 2.1). The thermally rejuvenated a-PS had a γ-process with an activation energy of 20.94 $\pm$ 8.75 kJ/mol, when after six

weeks of ageing the intensity of this process as well as its activation energy (23.64 ± 0.5 kJ/mol) increased. After one year of ageing, its intensity was increased more with an activation energy of 29.33 ± 0.3 kJ/mol. The activation energies of the γ-process have values lower but comparable to the ones in the study of Wypych et al.[34]. There, the authors state that the activation energy is about 35 kJ/mol for the thermally rejuvenated a-PS and increases to 45 kJ/mol after ten months of ageing at room temperature.

2.3.2 ATR-FTIR spectra

The bands in the 500-600 cm^{-1} region are due to out -of-plane deformation of the phenyl ring and they are conformationally sensitive[68,69]. The broad 538 cm^{-1} band due to amorphous components is assigned to the out-of-plane deformation mode of the phenyl ring in *trans*-conformation segments with four and more monomeric units[70]. The increase in *trans-trans* conformation between the rejuvenated and aged a-PS was confirmed by ATR-FTIR measurements. Figure 2.6 presents the peak intensity of normalized mid-infrared ATR-FTIR spectra of the thermally rejuvenated, short-term aged and long-term aged a-PS.

It is evident that the intensity of the 538 cm^{-1} band was increased during ageing, showing that the *trans-trans* conformation segments were also increasing in population with ageing.

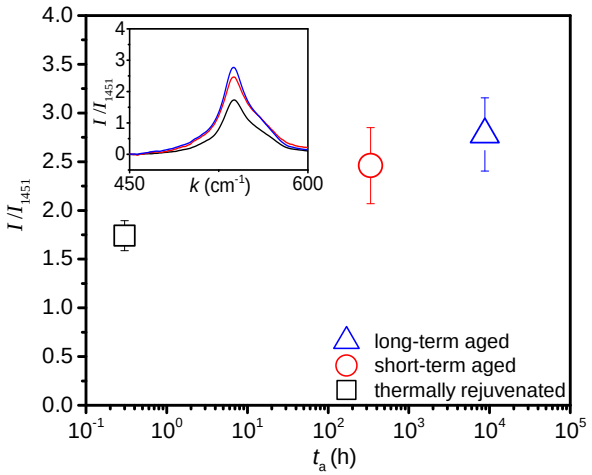

Figure 2.6: Normalized peak intensity (I/I_{1451}) of the *trans-trans* conformers for different treatments: thermal rejuvenation (black squares), short-term ageing (red circles) and long-term ageing (blue triangles) as a function of ageing time (t_a). Inset: Dependence of the normalized intensity (I/I_{1451}) as a function of wavenumber (k): thermal rejuvenation (black lines), short-term ageing (red lines) and long-term ageing (blue lines). Error bars: standard deviation of three measurements.

2.4 Discussion

To identify the molecular mechanism that links the emergence of a β^*-relaxation upon short-term ageing and its merging with the main α-relaxation, as well as the increase of intensity and activation energy of the γ-relaxation with long-term ageing, we discuss the findings of the previous sections in more detail.

Below the glass-transition region, manifested by the α-relaxation, a couple of relaxation processes are described in the literature: a β^*-process is detected directly below the main α-relaxation at around 47 °C (f = 110 Hz) for atactic polydisperse polystyrene and at around 67 °C (f = 110 Hz) for atactic monodisperse polystyrene, and is attributed to the rotation of the phenyl rings[41]. A non-cooperative α_s-relaxation is found in ultrathin a-PS films at around 10 °C (f = 0.7 Hz) which is attributed to surface dynamics[67]. The peculiar β_1- and β_2-relaxation processes (at about 90 °C and 180 °C, respectively, and f = 100 Hz) have been reported for a-PS with a solvent history and are attributed to the dynamics of helical "rods" formed by syndiotactic sequences[35]. A γ-process is detected at much lower temperatures (-120 °C, f = 100 Hz) and is assigned to torsional motion of methylene sequences formed in the backbone of the chain[41]. Time-of-flight and back-scattering studies suggest that the origin of this relaxation

is localized low-amplitude angular fluctuations[71]. Heading to even lower temperatures, the γ'- and δ-relaxations of PS may appear due to defects in chemical structure[41].

In this study, first of all, the α-relaxation appeared to have the same spectral shape (Figures 2.2, 2.3a,c,e and 2.4) and relaxation times in rejuvenated and aged samples. Isothermal ageing at 25 °C for six weeks resulted in an emergence of the peak of the β*-process (Figures 2.2, 2.3d,f and 2.4), as it was also seen by mechanical spectroscopy on PS and amorphous PEN[72]. This result contradicts a large amount of research which has shown a significant impact of ageing on the α-relaxation[73–76] at ageing temperatures close to the T_g. The reason behind this difference may be that this study is concerned with ageing at only low temperatures (T_g - 80 K). Hodge et al.[77] have already shown, by enthalpy relaxation experiments, that when ageing far below T_g, the enthalpy overshoot remains unaltered and a second endothermic peak is observed. More recently, Wypych et al.[34] have shown differential scanning calorimetry results for low-temperature aged PS, where the α-relaxation remains unaltered in the course of ten months, however these observations were not discussed. More proof about the insensitivity of the α-relaxation to low-temperature ageing has been seen in polymers[78] and metallic glasses[79], indicating that there are different mechanisms present to recover to equilibrium far from and close to T_g, specifically mentioning that

ageing far below T_g is disconnected from the α-process. Contrary, creep experiments on PS by Struik et al.[80] showed that PS ages in temperatures far below T_g, obeying time-temperature superposition. We believe that the results shown by Struik et al.[80] may display the macroscopic intertwined ageing kinetics of the β*- and α-processes as it has been observed by Van Breemen et al.[81]

Nevertheless, the reason for that the α-process seems to be insensitive to ageing in this study could be the complicated thermal history of the samples studied, which Struik named "downquench-storage-upquench" history[17]. Here, we rapidly quench the samples from a temperature above T_g to a temperature close to 0 °C, subsequently age the samples at room temperature, and then measure the samples by heating them with a rate of about 0.5 K/min. Heating the sample has an effect on the relaxation times: During heating, the samples age, their internal dynamics slow down with increasing ageing, and finally the history of the material may be (partly) erased by the heating scan at temperatures close to T_g. According to Struik,[17] fast processes exist that contribute to the volume relaxation which have a lower transition temperature than the T_g of the material. Consequently, when a material is heated, even at a temperature far below T_g, the physical ageing that has occurred can be partially erased[17]; the α-process observed seems not being affected by ageing. Furthermore, the dynamics delayed by ageing

may not be observed in the frequency window in which the measurements are done. Second, isothermal ageing at 25 °C for one year leads to the increase of intensity and the merge of the β*-process with the main α-process, in agreement with mechanical spectroscopy findings on PS[72]. Moreover, a very peculiar behavior can be seen for the β*-process (Figures 2.3d,f). The losses increase with increasing temperature from 55 °C to 70 °C. Increasing the temperature from 70 °C to 90 °C shows a decreasing trend of the losses. This behavior may be the evidence that at around 70 °C there is the transition temperature of the fast processes contributing to the volume relaxation as mentioned by Struik[17]. Heating above 70 °C, around 30 K below T_g of the material, the thermomechanical history of the specimen is already starting to be erased. Low-frequency Raman spectroscopy (LFRS) on a-PS[34] has shown that the Raman scattering around the Boson peak is weaker for aged samples at room temperature for ten months compared to the rejuvenated PS. The Boson peak was interpreted as an indication of more cohesive nano-domains surrounded by soft zones[34]. Decreasing intensity of the Boson peak was explained as decreasing contrast between the cohesive nano-domains and the soft surrounding medium (softer channels). Hence the decrease of the Boson peak intensity with ageing suggests that the glass nanostructure becomes more homogeneous[34]. The merge of the β*-process with the main α-relaxation upon long-term ageing could be rela-

ted to the decrease of mobility of the previously high mobility domains due to better packing. Having the LFRS picture in mind, one could interpret that these high mobility domains were "locked in" upon fast cooling, leading to no appearance of a β*- process in the dielectric spectrum (Figures 2.2, 2.3b and 2.4). We speculate that with short-term ageing, the domains of collective rearranging zones responsible for the main α-relaxation process develop into domains of high mobility for the more local sub-T_g relaxation motions, thereby "un-locking" the β*-process. Third, interestingly, also the γ-relaxation seems to be affected by ageing, as can be seen from its increase in both intensity and activation energy, as it was also seen in a previous study by dielectric spectroscopy on a-PS[34]. The comparison between the ATR-FTIR spectra for the 538 cm^{-1} band, which is representative of the *trans-trans* conformations, for the thermally rejuvenated, short-term aged and long-term aged a-PS is presented in Figure 2.6. Clearly, there is an intensity increase upon ageing, that implies an increasing number of *trans-trans*-conformers, which is in agreement with results reported for polycarbonate[82] and poly(L-lactide)[83]. Upon physical ageing of polycarbonate, it has been suggested that the *trans-cis* conformers rearrange into the *trans-trans* counterparts by comparing the spectral intensity of the characteristic bands[31,82,84]. The *trans-trans* conformations of polycarbonate are known to be energetically more stable than the *trans-cis* counterparts,

allowing closer packing of the polymer chains[85]. Similar tendencies of the conformational rearrangements from the high- to low-energy conformers upon physical ageing have also been reported for poly(ethylene terephthalate) (PET)[86], polystyrene (PS)[65], poly(vinyl chloride) (PVC)[87] and poly(L-lactide) (PLLA)[83]. It is suggested that the conformational changes which appear during physical ageing could lower the potential energy of a glassy polymer as it was discussed by Debenedetti and Stillinger[88].

2.5 Conclusions

Using broadband dielectric relaxation spectroscopy, the emergence of a β*-relaxation by short-term ageing and its intensity increase and merging with the α-process upon long-term ageing together was revealed for low-temperature aged a-PS for the first time by this technique. A progressive increase of the intensity and activation energy of the γ-relaxation was observed with ageing. By ATR-FTIR spectroscopy an –energetically favorable- increase of the *trans-trans* population was observed, upon ageing.

This suggests that the physical ageing favors the formation of low-energy molecular states, rationalized on the basis of the energy landscape concept. With rejuvenation and fast cooling, the system is falling into a local minimum, with relatively few *trans-trans*-conformers. Ageing leads the system

into ever deeper minima with increasing number of *trans-trans*-conformers.

Appendix

This appendix is concerned with the presentation of the ε'' data versus frequency in order to justify the lack of trustworthy fitting of the β*-process. In Figures A.1a, A.1b and A.1c, the dielectric loss ε'' for various temperatures is given for the β*-process. It can be seen that only the tail of this process appears in the studied experimental window, making the fitting of this process unreliable.

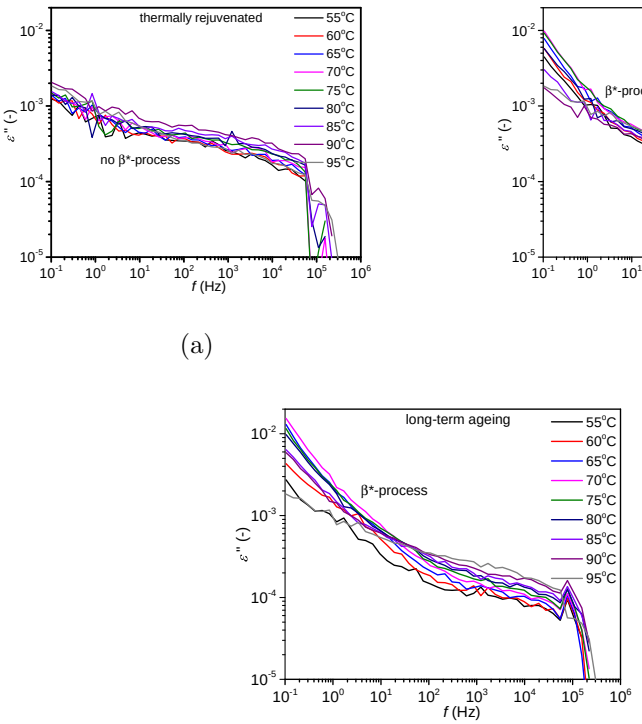

Figure A.1: Dielectric loss ε'' for various temperatures for (a) the thermally rejuvenated, (b) short-term aged and (c) long-term aged a-PS. The data were obtained by heating the sample from -120 °C to 145 °C at a heating rate of about 0.5 K/min. At each temperature, a frequency-sweep measurement was performed in the shown frequency range.

Chapter 3

Transient dynamics of cold-rolled and subsequently thermally rejuvenated atactic polystyrene

Abstract: The effect of plastic deformation on the molecular dynamics of atactic polystyrene (a-PS) was studied by broadband dielectric relaxation spectroscopy (BDRS), and complemented by attenuated total reflectance

This chapter is largely reproduced from: K. Grigoriadi, M. Wübbenhorst, L.C.A van Breemen, P.D. Anderson, M. Hütter. "Transient dynamics of cold-rolled and subsequently thermally rejuvenated atactic polystyrene using broadband dielectric spectroscopy". To be submitted.

Fourier transform infrared spectroscopy (ATR-FTIR) and polarized-light microscopy. The a-PS has been subjected to cold rolling, i.e. mechanical rejuvenation, followed by a quenching step (to arrest the deformed state) and thermal rejuvenation by heating above its glass-transition temperature, T_g. Cold rolling revealed in addition to the known α- and I(γ)-relaxations three additional, so far unknown relaxation processes (II, III and IV). Subsequent thermal rejuvenation suppresses the I-, II-, III-, and IV-relaxations. The ATR-FTIR results show the formation of T_2G_2 helices upon cold rolling. Polarized-light microscopy revealed the creation of oriented structures and internal stresses upon cold rolling, and their removal upon thermal rejuvenation. This work shows in a great extent the molecular differences between thermal and mechanical rejuvenation and helps to uncover the molecular mechanisms responsible for mechanical rejuvenation.

3.1 Introduction

One of the most fascinating subjects in condensed matter science is arguably the state of a glass. The frequent use of polymeric glasses in high-level applications, such as medical and aviation applications, makes understanding of their intrinsic mechanical response inevitable. Polymer glasses are out of equilibrium, and their evolution towards equilibrium is generally known as physical ageing[89]. The effect of physical ageing can be erased by increasing the temperature above the glass-transition temperature of the material, i.e. thermal rejuvenation[12]. It is also generally accepted that with deformation far beyond the yield strain, the dynamics of a polymer glass undergo changes that also lead to the erasure of physical ageing, a phenomenon called mechanical rejuvenation[12].

Thermally and mechanically rejuvenated glasses have similar macroscopic properties[13], however microscopically they may be rather different (e.g. anisotropy). A recent investigation on polymer glasses concluded that the thermally and mechanically rejuvenated glasses are in different states, and that mechanical deformation leads to an amorphous-amorphous phase transition[90]. Their results are confirmed by positron-annihilation life time spectroscopy experiments on a-PS and polycarbonate (PC). This idea has also been supported theoretically by other studies[91–93]. In his thorough re-

view on the subject of mechanical rejuvenation, McKenna[94] discussed the possible interpretations of the erasure of history of glassy materials with deformation below and above the yield point. At least close to T_g, the presented results of torsional dilatometry experiments prove that the free volume of the glass is not rejuvenated below the yield point[94]. Deformation above the yield point leads to a different DSC trace as compared to a thermally rejuvenated polymer, a sub-glass transition minimum is observed for the deformed polymer for which the molecular picture is not fully understood. McKenna suggests that deformation above the yield point in the polymer leads to a polyamorphic phase transition and not to rejuvenation[94].

Intriguing observations have been reported on density measurements on various cold-rolled glassy polymers[13,23]. Thermal rejuvenation is known to cause a decrease in the density, cold rolling, however, shows an increase in density.

Increased segmental mobility with mechanical deformation has been observed in various studies[26,28,95,96], and modeling studies argue that the increased segmental mobility is associated to different explored energy landscape regions in contrast to thermal rejuvenation[29,30].

The interpretation of increased mobility with deformation below the yield point should be discussed attentively. McKenna[94] indicates that the

glassy structure is independent of the mechanical stress. Specifically, evidence is provided that the mechanical equilibration time of a glassy material is not changed after mechanical perturbation. However, mechanical measurements cannot, possibly, be conclusive, since it is known that the equilibrium time scales are property dependent[97–99]. Mechanical stress below the yield point accelerates ageing and densifies the glass.

Time-strain superposition master-curves for polycabonate are different than the time-temperature master-curves, implying that temperature and strain influence the relaxation response of the glass in different ways[100]. O'conell et al.[100] states: "Because time-temperature superposition has been successful and deviations from it usually reported to be only subtle, our preliminary conclusion here is that the time-strain master-curve is not the correct master-curve. Further work needs to be done to establish the apparent validity of the time-temperature master-curve."

Regardless of the ongoing research concerning the effect of mechanical rejuvenation on mechanical and thermodynamical properties, there is little understanding from a microscopic viewpoint. Many techniques have been used to study the physical properties of mechanically deformed glass formers; nonetheless, only a minority can probe the dynamics in an extensive frequency range. Broadband dielectric spectroscopy is one of these few methods that can cover more than ten orders of magnitude in time-frequency.

Most attention has been paid to the study of glassy polymers during deformation[28,101] and is limited to the α- and β-transitions. Since a-PS is a material with rather low relaxation strength, studies using dielectric relaxation spectroscopy are challenging and hence sparse[34,102]. In this study, we report, for the first time, dielectric relaxation data on a-PS just after cold-rolling, and after subsequent thermal rejuvenation. Supporting ATR-FTIR spectroscopy and polarized-light microscopy studies connect the molecular dynamics with changes in the molecular structure of a-PS.

3.2 Experimental section

3.2.1 Materials

Atactic PS with the commercial name N5000 was kindly supplied in pellet form by Shell. The molecular weight and poly-dispersity index of the a-PS prior to rolling (M_w= 320.700 g/mol, PDI = 2.22) and after rolling (M_w= 319.200 g/mol, PDI = 2.23) were determined by High-Performance Liquid Chromatography (HPLC) using a Shimadzu HPLC instrument (Prominence -I, LC 2030C 3D). Within the accuracy of the equipment, no considerable differences in molecular weight and distribution were observed with cold rolling.

3.2.2 Sample preparation

The preparation of films (0.13 mm thickness) was performed by compression molding at 185 °C under vacuum. Initially, the pellets were compressed in three steps of rising pressure from ≈ 23 MPa up to ≈ 70 MPa. Thereafter, the mold was cooled down to room temperature at a pressure of approximately 23 MPa between two cold metal plates.

To further reduce the surface roughness, the acquired films were recompressed between two Kapton foils at 185 °C at ≈ 70 MPa for ten minutes under vacuum. Eventually, the specimens were cooled down to room temperature at ambient pressure.

3.2.3 Treatments

Cold rolling of the a-PS films was performed by rolling in a Durston DRM C100 two-roll mill (diameter of rolls 50 mm) until the thickness of the films was reduced by 20% to 30% of their initial thickness. The samples were then (i) introduced into the dielectric sample cell at a temperature of ≈ -100 °C in order to arrest their cold-rolled state and (ii) heated above their T_g (thermal rejuvenation) and then cooled down with a rate of 3 K/min.

3.2.4 Broadband dielectric relaxation spectroscopy (BDRS)

Employing a high-precision dielectric ALPHA analyzer (Novocontrol Technologies) connected to a Novocontrol Quatro temperature system keeping control of the specimen temperature (≤ 0.05 K), dielectric measurements were performed from -130 °C to 180 °C in a continuous frequency-sweep mode from 10^0 Hz to 10^6 Hz, while a temperature ramp at 3 K/min was employed in both heating and cooling stages. The specimens (20 mm in diameter and thickness of ≈ 60 μm) were clamped between brush-plated stainless steel electrodes.

The imaginary part of the empirical Havriliak-Negami (HN) relaxation function[64] was used to determine the relaxation time $\tau(T)$ and other relaxation parameters by fitting the dielectric loss spectra $\epsilon''(\omega)$ acquired at various temperatures,

$$\epsilon'' = -\mathrm{Im}\left\{\frac{\Delta\epsilon}{(1+(i\omega\tau)^a)^b}\right\} + \frac{\sigma}{\epsilon_\nu\omega}, \tag{3.1}$$

where $\Delta\epsilon$ denotes the relaxation strength, while a and b ("shape parameters") relate to the logarithmic slope of the low-frequency loss tail (a) and the high-frequency loss tail (ab). The last term stands for Ohmic conduction, with conductivity σ, vacuum permittivity ϵ_ν and angular frequency $\omega = 2\pi f$. A thorough description of the analysis of dielectric data

can be found in the work of Wübbenhorst et al.[63] and Van Turnhout et al.[64].

3.2.5 Attenuated total reflection Fourier transform infrared spectroscopy (ATR-FTIR)

The a-PS films were measured in the range of 400-4000 cm^{-1} at a resolution of 4 cm^{-1} and a total of 20 scans with a FTIR PERKIN ELMER Spectrum Two spectrometer in reflection mode. Two measurements were performed on each sample. For analysis of the data, the baseline-corrected spectra were normalized with the 1451 cm^{-1} peak which is conformationally insensitive and therefore used as internal standard. The difference spectrum was obtained by subtraction of the spectrum of the not-rolled from the cold-rolled specimens.

3.2.6 Polarized-light microscopy

Polarizing-light microscopy measurements (Zeiss Axio Imager D1) were performed for observing the internal stresses of the samples. The morphology is captured by a Zeiss AxioCam MRc 5 camera.

3.3 Results

3.3.1 Dielectric relaxations

Figures 5.1 and 5.2 show the effect of cold rolling and subsequent quenching to a temperature of approximately -100 °C on the molecular dynamics of a-PS. Five processes are detected which are named in order of increasing temperature. First, at -100 °C at 122 Hz the γ-relaxation (I) is observed. Heading towards higher temperatures, at 122 Hz, the II- and III-processes occur at -60 °C and 18°C, respectively. A IV-transition appears at around 75 °C (122 Hz) and the α-transition around 120 °C at 122 Hz. Although the primary α-relaxation and the γ-process (I) are reported in earlier studies, the other identified processes (II, III, and IV) have not been mentioned in literature before. The relaxation-time data, calculated by the fit of isothermal spectra $\epsilon''(\omega)$ to Equation 3.1, are shown in the Arrhenius diagram, see Figure 5.3. The main α-process, well-known by its distinctive curvature in the temperature dependence of the relaxation time, $\tau(T)$, was fitted to the Vogel-Fulcher-Tamman (VFT) law[102],

$$\tau = \tau_\infty \exp\left(\frac{E_\mathrm{V}}{R(T - T_\mathrm{V})}\right), \tag{3.2}$$

with E_V and T_V the Vogel activation energy and the Vogel temperature, respectively. The parameters R and τ_∞ are the universal gas constant and the ultimate relaxation time.

All processes except the primary α-process show Arrhenius-like behavior, each with different activation energies, E_A, according to:

$$\tau = \tau_\infty \exp\left(\frac{E_A}{RT}\right). \tag{3.3}$$

The fit parameters for the five relaxations are listed in Table 5.1. The five processes detected can be classified as follows: Starting from the lowest temperature (Figures 5.1a, 5.2), the I-process has an activation energy of 33.8 kJ/mol (Figure 5.3) characteristic for a local process[34]. At a somewhat higher temperature, process II has an activation energy of 60 kJ/mol (Figure 5.3). Around 18 °C (at 122 Hz) the III-process is spotted (Figures 5.1a, 5.2) with an activation energy of 76.6 kJ/mol (Figure 5.3). Heading to higher temperatures, at around 60 °C to 70 °C the IV-process emerges, but disappears just after passing 70 °C by shifting towards lower frequencies (implying a negative activation energy), which goes simultaneous with a fading out of process III (Figure 5.3). The main α-relaxation follows a VTF-behavior, characteristic for segmental mobility (Figure 5.3). Heating the sample above its glass transition, i.e. thermal rejuvenation, leads to

Table 3.1: Activation parameters and their standard deviation for the α-process found in a-PS for different treatments. The error of T_V is not mentioned because it is small (order of magnitude: 10^{-3} K).

	α-process		
treatment	$\log(\tau_\infty[s])$	E_V(kJ/mol)	T_V(K)
cold-rolled	-9.65±0.02	5.21±0.1	345.9
rejuvenated /measured while cooling	-11±0.12	7.48±0.6	343.9

Table 3.2: Activation parameters and their standard deviation for the I, II and III processes found in cold-rolled a-PS.

process	$\log(\tau_\infty[s])$	E_A(kJ/mol)
III	-16.2±0.2	76.6±0.8
II	-17.8±0.6	60.6±3.1
I	-13.8±0.1	33.8±0.6

the removal of the thermo-mechanical history of the sample and the development of different molecular dynamics consisting of two "usual" relaxation processes, namely the primary α-relaxation and γ-relaxation processes (Figures 5.1b, 5.2). This thermally rejuvenated sample has higher Vogel activation energy E_V as compared to the cold-rolled one (Table 5.1). The γ-process is again weak in intensity and hence did not allow for a reliable quantitative analysis.

The commonly used Arrhenius analysis provides us with information on the activation energies of the new processes but due to complexity of these processes it is difficult to proceed to a microstructural interpretation[103]. A

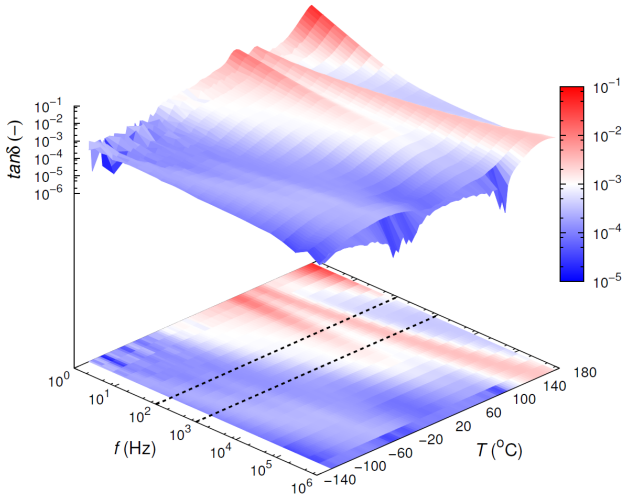

(a)

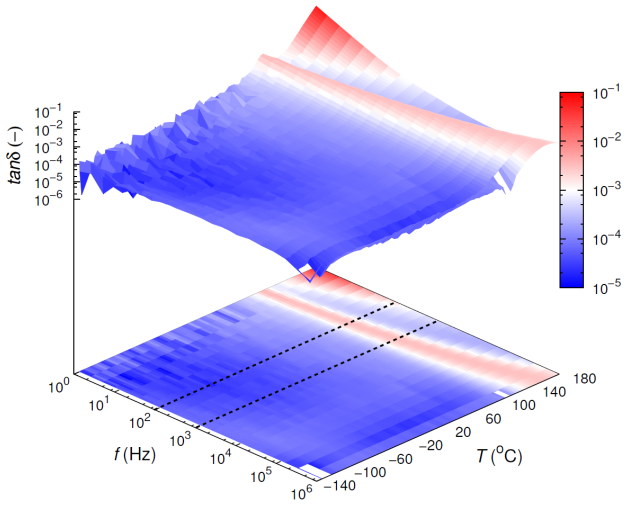

(b)

Figure 3.1: Three-dimensional representation of the dielectric loss-tangent $\tan\delta(f, T)$ for (a) the cold-rolled and (b) subsequently thermally rejuvenated a-PS. The dashed lines correspond to the spectra shown in Figure 5.2.

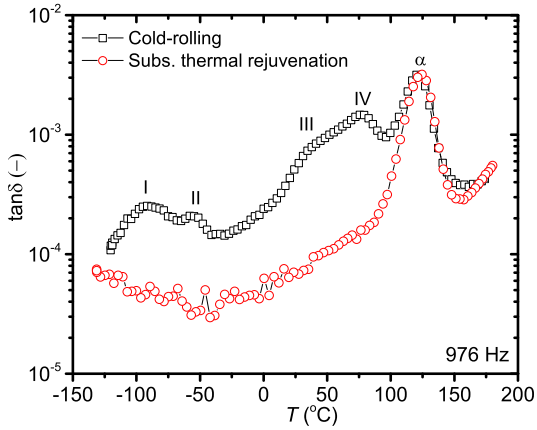

(a)

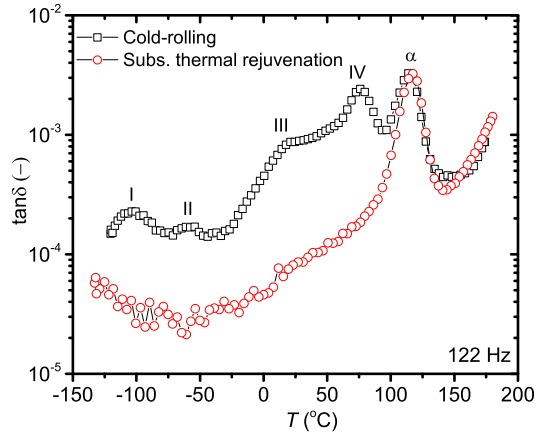

(b)

Figure 3.2: Dielectric spectra of tanδ vs. temperature as measured at frequencies of 976 Hz (a) and 122 Hz (b) for the cold-rolled a-PS (squares) versus the subsequently thermally rejuvenated a-PS (circles). The data correspond to the dashed lines in Figure 5.1.

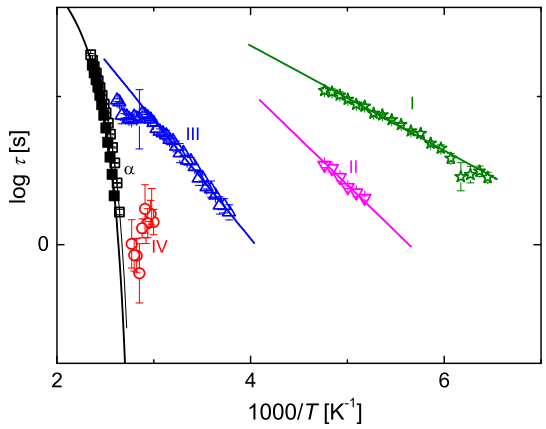

Figure 3.3: Activation diagram showing the relaxation times τ_α, τ_{IV}, τ_{III}, τ_{II}, and τ_I for the cold-rolled a-PS (open symbols), and activation diagram showing the relaxation times τ_α for the thermally rejuvenated sample (filled symbols). Lines are fitting lines. The I(γ)-process of the thermally rejuvenated sample is not shown due to the noisy signal.

more comprehensive way to analyze these relaxations is given by their activation entropies (ΔS) and activation enthalpies (ΔH^*), using the analysis described by Starkweather[103]. Table 3.3 shows the values for ΔH^* and ΔS for the III-, II- and I(γ)-relaxations of cold-rolled a-PS.

Now, starting from low temperatures, it appears that the I(γ)-relaxation has a ΔS of 0.0173 kJ/(mol K), very close to zero, implying a non-cooperative motion[103]. The II-relaxation and the III-process have a higher ΔS; 0.0922 kJ/(mol K) and 0.0583 kJ/(mol K), respectively, that may be interpreted

Table 3.3: Activation parameters (ΔH^* and ΔS) and T' fitted according to Starkweather's procedure[103] for the I, II, and III-processes found in cold-rolled a-PS.

relaxation	T' (K)	ΔH^* (kJ/mol)	ΔS (kJ/(mol K))
III	259.52	61.45	0.0583
II	185.62	43.44	0.0922
I	136.09	31.50	0.0173

as an increased cooperativity[103].

3.3.2 ATR-FTIR spectra

Figure 5.4 exhibits the normalized and difference infrared ATR-FTIR spectra for a-PS before and after cold rolling. The negative bands in the difference spectrum are connected to the vibrational modes of the main chain at 2848 cm^{-1} (CH_2 symmetric stretching)[104,105] and 2923 cm^{-1} (CH_2 asymmetric stretching)[104,105]. The positive bands are associated with the phenyl groups. Two bands that change considerably with cold rolling are the bands appearing at the difference spectrum at around 538 cm^{-1} and 754 cm^{-1} which show a positive change. The 538 cm^{-1} band is associated with the δ-form helical structure of syndiotactic polystyrene[106–108] which is considered to be a short helix consisting of 7-12 monomeric units[109]. The 754 cm^{-1} band is also considered to be associated with δ-form helices[108]. These helices are formed by T_2G_2 conformational sequences[110–112].

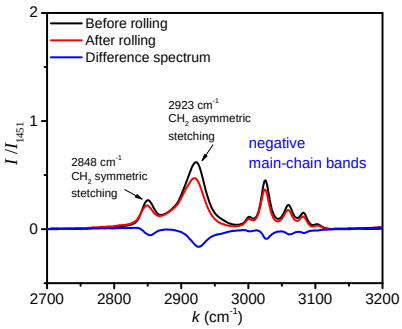

(a)

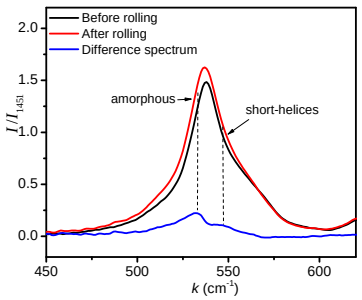

(b)

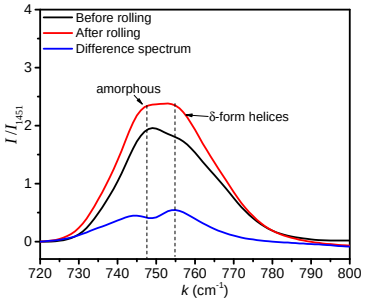

(c)

Figure 3.4: (a) Normalized peak intensity (I/I_{1451}) ATR-FTIR spectra of a-PS before rolling (black line), after rolling (red line) and their difference spectrum (blue line); and spectra focused on (b) conformationally sensitive region 450-620 cm^{-1} and (c) 720-800 cm^{-1}.

3.3.3 Polarized-light microscopy

In Figure 5.4, the polarized-light microscopy photos for a-PS subjected to cold rolling (Figure 5.4a) and subsequent thermal rejuvenation (Figure 5.4b) are shown. The effect of cold rolling on the creation of orientation and internal stresses in the polymer is observed by the color pattern under polarized light. Thermal rejuvenation erases the internal stresses of the a-PS films, as can be seen in Figure 5.4b.

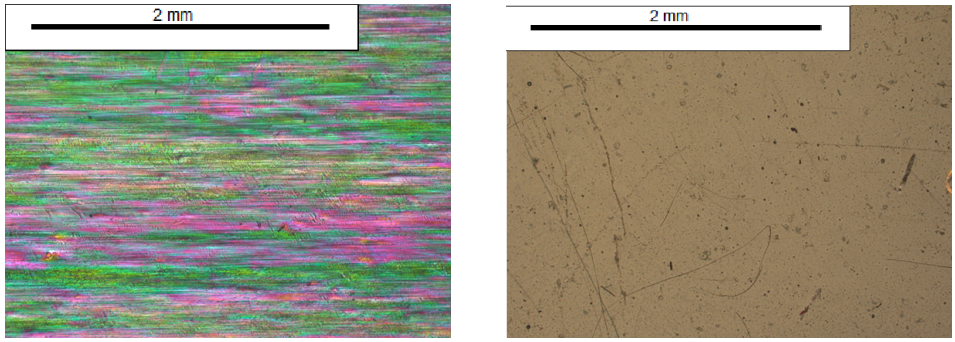

(a) (b)

Figure 3.5: Polarized-light microscopy photos of a cold-rolled a-PS film (a) versus a subsequently thermally rejuvenated film (b). When no stresses are observed for the rejuvenated sample, the orientation and internal stresses due to cold rolling on the film is evident.

3.4 Discussion

By the results presented above, yet unknown dynamics of cold-rolled a-PS, a polymer heavily used in industry and broadly investigated in academia, have been uncovered. To classify the molecular processes of a-PS caused by cold rolling, the results are discussed in more detail in the following. A general picture of the processes is also proposed in Figure 5.6, and discussed in the following.

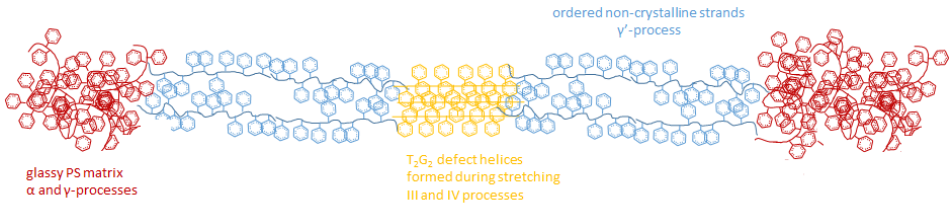

Figure 3.6: Proposed model for the relaxation processes of cold-rolled a-PS.

(a) **γ-process (I).** At the lowest temperatures measured, a γ-process is observed (-104 °C at 122 Hz) (Figures 1-a, 2, 3) with an activation energy of 33.8 kJ/mol (Table 5.1) representative of the γ-relaxation of a-PS[34] which is claimed to be localized low-amplitude motions[71]. This process also has an enthalpic barrier (ΔH^*) of around 31.50 kJ/mol and an entropic barrier (ΔS) of 0.0173 kJ/(mol K) which is close to zero, hence, representative of a non-cooperative relaxation mechanism[103,113].

(b) **γ'-process (II).** Progressing towards higher temperatures, an unknown II-process appears. This process appears at around -60°C (at 122 Hz) and is observed in a broad frequency range (10^1 - 10^5 Hz) (Figure 5.1a, 5.2). Its activation energy of 60.6 kJ/mol (Table 5.1) is common for phenyl-ring rotation[34], but the temperature/frequency where it appears is non-standard. The fact that $\Delta H^* = 32.44$ kJ/mol is similar to the ΔH^* of the γ-process, showing that the same rotational-potential contributions are involved, implies that the I (γ)- and II-processes are similar in nature, so, from now-on the II-process will be called γ'. In contrast to the γ-process, the γ' has a higher activation entropy ($\Delta S = 0.0922$ kJ/(mol K)), that could imply that there is more cooperativity in this relaxation[103]. This higher entropic barrier is probably due to the stretched chains as it is confirmed by polarized microscopy (Figure 5.5) and the negative difference spectrum, obtained via FTIR, of the vibrations connected to the symmetric and asymmetric stretching of main-chain bands (Figure 5.4).

(c) **III-process.** Heading to higher temperatures, a broad and strong III-relaxation is observed (-26 °C to 40 °C at 122 Hz) (Figures 5.1a, 5.2) with an activation energy of around 76.6 kJ/mol (Table 5.1). This unfamiliar process has a similar activation energy as the β_1- and β_2- processes found in a-PS and s-PS. These were attributed to the defect mechanism of kink inversion of T_2G_2 helices[102]. Despite the very similar activation

energy, the process III is about two (four) decades faster than the β_1- (β_2) processes. In our study, there are indications of T_2G_2 helices, see the difference spectrum ATR-FTIR, suggesting that kink inversion of syndiotactic helices is the molecular mechanism behind process III.[102] An explanation for the high activation energy and substantial activation entropy of process III is a relaxation mechanism involving T_2G_2 helices. Considering the findings on oriented fibrilar material reported by Li et al.[114], we speculate that the observed helices in the ATR-FTIR spectra (Figure 5.4) together with the highly activated III-process may be due to the highly stretched (*trans-trans*) fibrils with a crystal-like packing. Additional evidence for this idea comes from the surprising similarity between the activation parameters of process III ($\Delta H^* = 61.45$ kJ/mol and $\Delta S = 0.0583$ kJ/(mol K)), respectively, and the α_c known from semicrystalline LDPE[66] (Table 3.4), which has an activation enthalpy of 64.71 kJ/mol and a high, but different activation entropy (0.20 kJ/(mol K)). This strong analogy favors the picture of a kink propagation process within a locally crystalline packing of *trans*-sequences of regioregular PS within the fibrils, see Figure 5.6.

With the removal of strain softening glassy polymers display ductile behavior[115,116]. The presence of defects in crystals of i-PP (isotactic polypropylene) creates high ductility and flexibility because of polymorphic transformations that occur during deformation[117]. By combining these two

Table 3.4: Activation parameters of the ΔS and ΔH^* for the III-process and α_c found in cold-rolled a-PS and LDPE respectively[66].

relaxation	T (K)	E_A (kJ/mol)	ΔH^* (kJ/mol)	ΔS (kJ/(mol K))
III a-PS	259.52	76.57	61.45	0.0583
α_c LDPE	185.62	119.6	64.71	0.2012

observations, we propose that a similar mechanism is responsible for the ductile behavior of mechanically rejuvenated PS in which, during deformation, the *trans-trans* (amorphous) sequences are forming short-length defect helices that create the macroscopically observed flexibility. The proposed schematics on the molecular origins of this process are depicted in Figure 5.6.

(d) **IV-process.** At even higher temperatures, a new dielectric IV-process appears (Figures 5.1a, 5.2) below the α-transition and at exactly the point where the III-process starts to vanish at 70 °C. While in its low-temperature part it has a high positive E_A, at around 70 °C the relaxation seems to shift towards low frequencies together with a strong decrease in its intensity, similar to a melting transition. A series of custom-made deformation calorimetry (DC) experiments[22] on glassy polymers such as polystyrene (PS), polycarbonate (PC) and poly (methyl methacrylate) (PMMA) revealed that plastic deformation below the glass transition results in high internal energy storage, that is released upon heating of the sample and

appears as an exothermic abnormality in the region below T_g in DSC[21,22]. Molecular dynamic simulations[95] also observed that the stored internal energy in PS and PC glasses after plastic deformation is remarkably high. Such behavior is explained in terms of localized shear transformation zones (STZ's)[118]. We think that the IV-process represents the stored energy of the highly stretched fibrils. Upon heating, the fibrils collapse because of softening of the a-PS glassy matrix just below its T_g, dissipating the absorbed energy.

(e) **Primary α-relaxation process.** The α-process shows a lower activation energy (5.21 kJ/mol) upon cold rolling, in comparison to the α-process (7.48 kJ/mol) of a thermally rejuvenated specimen (Table 5.1). It has been observed by dielectric spectroscopy measurements during tensile deformation that cold rolling accelerates the α-process, of a poly(vinyl chloride) glass[28]. Also a stretched polycarbonate (PC) has shown increased molecular mobility[101] as compared to its non-deformed counterpart. Optical photobleach experiments on poly(methyl methacrylate) (PMMA) showed also an increase in segmental mobility during deformation[96]. In our data, the lower activation energy appearing for the cold-rolled a-PS could imply that the molecular packing is constrained less, resulting in a less abrupt activation of the primary α-process. Subsequent thermal rejuvenation returns the molecular dynamics to what it was prior to mechanical defor-

mation: here, only the α- and γ-processes are notable, with the α-process having an increased activation energy and the γ-process becoming much broader.

3.5 Conclusions

Using dielectric relaxation spectroscopy, three new relaxation processes after cold rolling and quenching of atactic polystyrene, i.e. II, III and IV, are unveiled for the first time. Subsequent thermal rejuvenation suppresses all these new processes except for the main α-transition and the weak γ-transition. ATR-FTIR difference spectroscopy suggests the existence of short-defect T_2G_2 helices formed due to cold rolling. Polarized-light microscopy shows the formation of an oriented structure via visualization of internal stresses. We speculate that the new relaxation processes are due to the formation of the short-defect T_2G_2 helices (III- and IV-processes) as a result of plastic deformation, and that, upon heating, these helices collapse because of softening of the a-PS glassy matrix just below its T_g, dissipating the absorbed energy (IV-process).

Our results reveal significant differences in the molecular dynamics between thermally and mechanically rejuvenated glassy a-PS. A possible mechanism behind the macroscopic ductility of mechanically rejuvenated sam-

ples is proposed. Our findings could be corroborated via other experimental techniques to obtain more information on mechanisms underlying the mechanical rejuvenation, e.g. X-ray scattering or nuclear magnetic resonance spectroscopy. Moreover, in the context of molecular dynamic simulations, our findings suggest that the initial conditions should be carefully chosen, taking into account the spatial heterogeneities.

Chapter 4

Dynamics of cold-rolled and subsequently aged atactic polystyrene

Abstract: The molecular dynamics of cold-rolled and subsequently aged at 50 °C atactic polystyrene (a-PS) were studied by broadband dielectric relaxation spectroscopy (BDRS). Additional attenuated total reflec-

This chapter is largely reproduced from: K. Grigoriadi, M. Wübbenhorst, L.C.A van Breemen, P.D. Anderson, M. Hütter. "Dynamics of cold-rolled and subsequently aged atactic polystyrene studied by means of broadband dielectric relaxation spectroscopy". To be submitted.

tance Fourier transform infrared (ATR-FTIR) experiments were performed. While for a cold-rolled sample I(γ)-, II(γ')-, III-, IV- and α-relaxations were observed (Chapter 3), subsequent ageing causes a decrease in intensity of all relaxations, a merging of the γ- and γ'-relaxations and suppression of the III-relaxation. The main α-relaxation shows an increased Vogel activation energy with ageing. The ATR-FTIR results show a decrease of the *trans-trans* conformers upon ageing. Ageing after cold rolling is signified by a return of the structure in a more isotropic state.

4.1 Introduction

The physics of polymer glasses is studied intensely for years. More specifically, great attention has been paid to the evolution of the out-of-equilibrium glass towards equilibrium, a phenomenon known as "physical ageing" [8]. Heating the glass above its glass-transition temperature is known to erase the structural changes caused by physical ageing, a phenomenon called "thermal rejuvenation" [12]. Yet, it has also been acknowledged that also large stresses can remove the thermomechanical history of the material, i.e. "mechanical rejuvenation" [12].

It has been speculated that thermally and mechanically rejuvenated glasses have similar ageing mechanisms [89]. Contrarily, there is a large amount of investigations that show that these two types of ageing are different in nature [14,21,90,119]. Creep tests on thermally vs. mechanically rejuvenated a-PS and PC have shown that the creep compliance for the mechanically deformed specimens increases three times faster in time than the thermally rejuvenated samples, indicating a higher segmental mobility [13]. Differential scanning calorimetry (DSC) measurements on PS revealed a fundamental difference for the mechanically deformed a-PS [21], PVC [119] and other glassy polymers [14]; an exothermic peak was observed below the glass-transition temperature, indicative of stored internal energy which relaxes

with time. Positron-annihilation life time spectroscopy (PALS) on PS and PC[90] shows that the free volume hole time-evolution is different for the mechanically deformed specimens in comparison to the thermally rejuvenated specimens. A large amount of direct microscopic studies indicate that plastic deformation leads to a heterogeneous structure in the whole volume of a glassy polymer[14]. Volynskii et al.[14] concluded in their extended literature review on the structural aspects of physical ageing of polymer glasses, that the mechanically deformed glassy polymers contain shear bands filled with oriented fibrillar material of low density; they speculated that these bands are the primary cause for the different observed features due to subsequent ageing. Sub-yield large deformations at temperatures below T_g cause densification of the glassy material and lead to accelerated ageing[12]. In summary, the research in literature hints at differences between ageing after thermal and mechanical rejuvenation, however there is limited insight from a molecular point of view. One of the techniques that can offer significant insight on the molecular mechanism responsible for the ageing after deformation is broadband dielectric relaxation spectroscopy (BDRS), which has a significant advantage over many other techniques: it can explore the dynamics over an extensive frequency range. The majority of studies with BDRS is done on thermal rejuvenation and ageing[34] and during deformation of polyvinyl chloride (PVC) and polycarbonate (PC)[28,101] primarily.

Since a-PS is a low-capacitance material, BDRS research on this material is scarce[34,102].

The goal of this study is to examine the effect of ageing on the molecular dynamics of cold-rolled a-PS by BDRS. Additionally, ATR-FTIR spectroscopy measurements are performed to relate the change of the molecular dynamics with changes in the molecular rearrangements of a-PS.

4.2 Experimental section

4.2.1 Materials

Atactic PS (N5000) was kindly supplied in form of pellets by Shell. The molecular weight (M_w = 320.700 g/mol) and poly-dispersity index (PDI = 2.22) were determined by High-Performance Liquid Chromatography (HPLC) using a Shimadzu HPLC instrument (Prominence -I, LC 2030C 3D).

4.2.2 Sample preparation

The a-PS pellets were compression molded at 185 °C under vacuum in steps of increasing pressure from ≈ 23 MPa and up to ≈ 70 MPa. Films of about 0.1 mm thickness were prepared which cooled down to room temperature

between two cold metal plates at a pressure of about 23 MPa. The obtained films were recompressed between two Kapton films at a pressure of about 75 MPa and temperature of 185 °C under vacuum for ten minutes to decrease their surface roughness. Finally, the samples were cooled down to room temperature.

4.2.3 Treatments

The a-PS films were cold rolled in a Durston DRM C100 two roll mill (diameter 50 mm) and their thickness was reduced by 20% to 30%. Two treatments were applied to the specimens: (i) directly after cold rolling, the specimens were introduced in the frozen dielectric chamber ($\approx$ -100°C) to capture their cold-rolled state, and (ii) aged for three hours at 50 °C in a nitrogen atmosphere.

Broadband dielectric relaxation spectroscopy (BDRS) and attenuated total reflectance Fourier transform infrared spectroscopy (ATR-FTIR)

BDRS: Specimens of 20 mm in diameter and thickness of about 70 μm were placed between brush plated stainless steel electrodes. Dielectric measurements were conducted in a temperature range from -130 °C to 180 °C in a frequency-sweep mode from 10^0 Hz to 10^6 Hz. ATIR-FTIR: Measurements

were performed in the range 400-4000 cm^{-1} at a resolution of 4 cm^{-1} and a total of 20 scans. The normalization of the spectra was carried out with the 1451 cm^{-1} peak which is conformationally insensitive and therefore used as internal standard. The detailed analysis protocols for BDRS and FTIR have been discussed in Chapter 3.

4.3 Results

4.3.1 Dielectric relaxations

BDRS measurements were performed to study the molecular dynamics of cold-rolled and subsequently aged a-PS.

In Figures 4.1 and 4.2, the relaxation behavior is depicted for a-PS that is cold-rolled and cold-rolled and subsequently aged at 50 °C. The five relaxation processes observed for the cold-rolled sample are described in our previous study (Chapter 3). A short summary of these processes is given for convenience, in order of increasing temperature and at a frequency of 122 Hz: I(γ)-relaxation at -100 °C, II(γ')-process at -60 °C, III-process at 18°C, IV-transition around 75 °C and the α-relaxation at 120 °C. In contrast, the results for the cold-rolled and subsequently aged for three hours at 50 °C a-PS measured at frequencies 122 Hz and 976 Hz are depicted

in Figure 4.2. The spectra show the segmental α-relaxation process at approximately 120 °C and a broad peak at approximately 65 °C. In view of Figure 4.2, this latter peak is the same in nature as the IV-process of the cold-rolled and quenched material. The quantitative analysis of the dielectric data is described in our previous work (Chapter 3). The fit parameters for the α-relaxation for the cold-rolled and cold-rolled and aged a-PS are presented in Table 4.1. The I(γ)-process of the aged sample has a too low intensity and thus does not permit for a quantitative analysis. Also, in the case of the IV-process, the data is not accurate enough to allow quantitative characterization. In Figure 4.3, the activation map of a-PS subjected to the different treatments is plotted. Clearly, ageing has a substantial effect on the molecular dynamics of a-PS. The α-relaxation shows an increase in activation energy with ageing (Table 4.1). Heading to lower temperatures, the IV-transition appears broader with less intensity (Figure 4.2). Progressing to even lower temperatures, the suppression of the III-process is evident. Finally, the II(γ')- and I(γ)-processes merge and appear significantly broader and with lower intensity, close to the noise level.

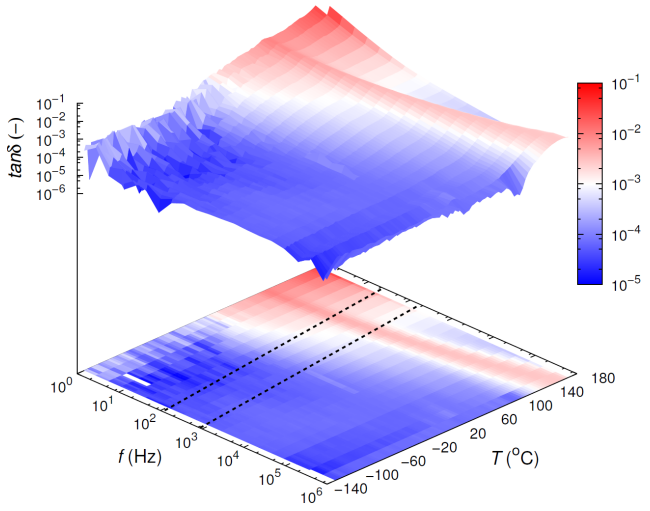

Figure 4.1: Three-dimensional representation of the dielectric loss tangent $\tan\delta(f, T)$ for the cold-rolled and subsequently aged a-PS. The dashed lines correspond to the spectra shown in Figure 4.2.

Table 4.1: Activation parameters and their standard deviation for the α-process found in a-PS for different treatments. The error of T_V is not mentioned because it is small (order of magnitude: 10^{-3} K).

	α-process		
treatment	$\log(\tau_\infty[s])$	E_V(kJ/mol)	T_V(K)
cold-rolled (Chapter 3)	-9.65±0.02	5.21±0.1	345.9
cold rolled and aged	-10.71±0.22	7.35±1.1	337.2

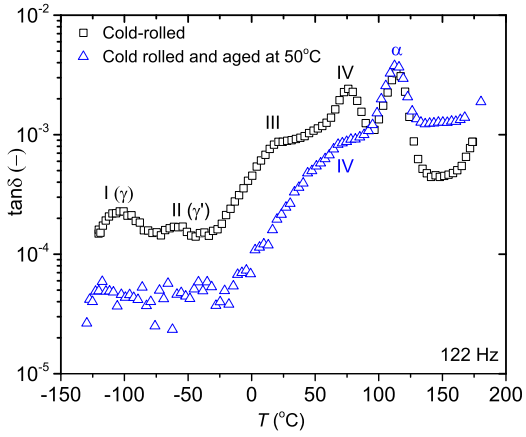

(a)

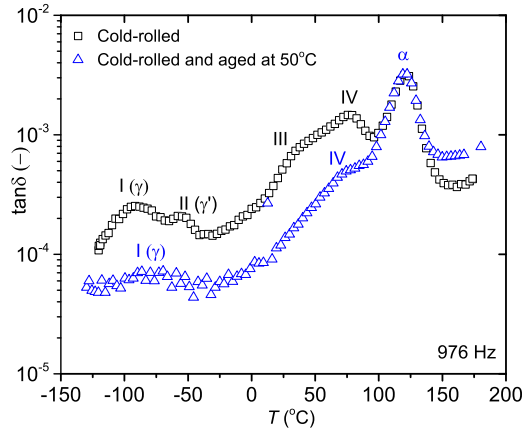

(b)

Figure 4.2: Dielectric spectra of tanδ versus temperature as measured at a frequency of 122 Hz (a) and 976 Hz (b) for the cold-rolled a-PS (squares) (reproduced from Chapter 3) versus the cold-rolled and subsequently aged a-PS (triangles). The data correspond to the dashed lines in Figure 4.1.

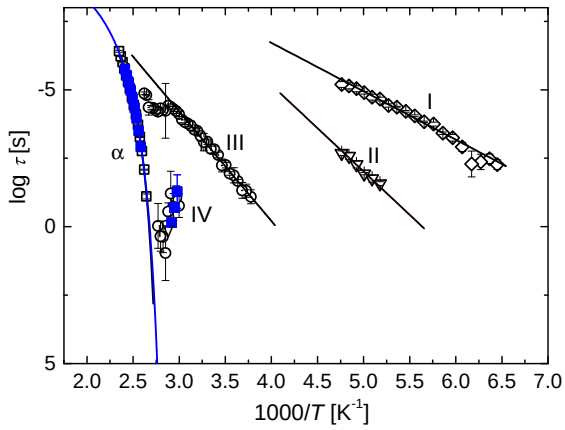

Figure 4.3: Activation diagram showing the relaxation times τ_α, τ_{IV}, τ_{III}, τ_{II} and τ_I for the cold-rolled a-PS (open symbols) (reproduced from Chapter 3) and activation diagram showing the relaxation times τ_α and τ_{IV} for the subsequently aged sample (filled symbols).

4.3.2 ATR-FTIR spectra

The normalized infrared ATR-FTIR spectra of cold-rolled and subsequently aged a-PS are presented in Figure 4.4. Ageing after mechanical rejuvenation increases slightly the main-chain vibrations (Figure 4.4a) and decreases the intensity of the *trans-trans* conformers located in the 538 cm^{-1} band. The 754 cm^{-1} band, associated with δ-form helices[108], is also decreased.

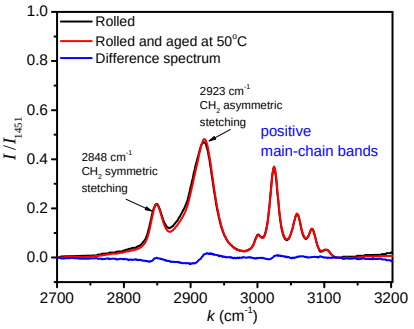

(a)

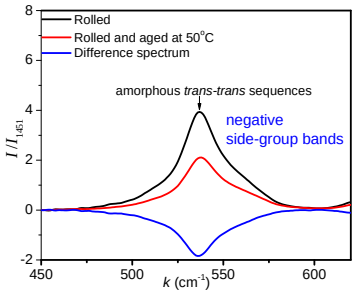

(b)

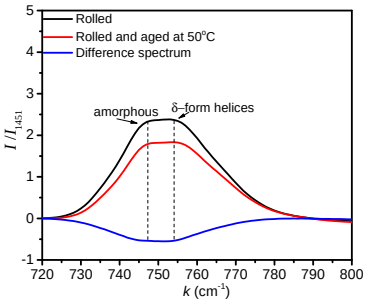

(c)

Figure 4.4: Normalized peak intensity (I/I_{1451}) ATR-FTIR spectra of cold rolled a-PS (black line), cold rolled and subsequently aged (red line) and their difference spectrum (blue line). Spectra focused on the region (a) 2700-3200 cm^{-1}, (b) conformationally sensitive region 450-620 cm^{-1} and (c) 720-800 cm^{-1}.

4.4 Discussion

Considering the presented data on the molecular dynamics of cold-rolled and subsequently aged a-PS, we discuss about the possible molecular mechanisms behind the BDRS observations.

The I(γ)- and II(γ')-processes spotted at about -104 °C and -60 °C at a frequency of 122 Hz (Figures 4.1-4.2) lose intensity and merge into one process during ageing. This process is argued to represent restricted low-magnitude motions[71]. While the mechanism by which this merging happens remains to be resolved, it is clear that ageing of the cold-rolled a-PS has a profound effect on the γ-relaxation. The III-process observed for a freshly cold-rolled a-PS at a temperature of -18 °C is suppressed with ageing, while the IV-process, observed for a freshly cold-rolled a-PS at 60-70 °C (at 122 Hz) is decreased in intensity with ageing. To establish the molecular mechanism behind the merging and hindering of these relaxations, one should recall the proposed mechanism responsible for these processes, see Chapter 3. In our previous study, we speculated that the I(γ)- and II(γ')-processes may be due to the isotropic-amorphous phase and the oriented-amorphous state, respectively. The merging of these two relaxations together with the decrease of the *trans-trans* population, representative of orientation of the chains, makes evident the loss of orientation

of the chains in the polymeric matrix. Moreover, in Chapter 3, we speculated that the III- and IV-processes may be due to formed defect helices in highly stretched oriented fibrils. Subsequent ageing of the cold-rolled sample for three hours at 50 °C suppresses the III-process and decreases the intensity of the IV-process (Figure 4.2).

Various studies[120,121] have shown that the oriented fibrillar material is healing in the course of time. Berger et al.[120] investigated the polymer mobility within the fibrillar material via thermally stimulated depolarization currents on PS and brominated PS (PBrS). They concluded that ageing at temperatures between 10-20 °C below T_g leads to partial healing of the fibrillar material. Yang et al.[121] applied low-angle electron diffraction (LAED) to investigate the geometrical characteristics of fibrils. They concluded that during ageing of PS at room temperature the fibrils coalesce. Therefore, we speculate that the suppression of the III-process and the intensity loss of the IV-process is due to partial fibril-healing. The decrease of the dielectric loss tangent ($\tan\delta$) (Figure 4.2), shows the decrease in mobility of the system with ageing, while the broadening of peaks shows the structural heterogeneity involved in the system[122]. In their extensive work, Salamatina et al.[22] observed in differential scanning calorimetry experiments (DSC) that, while a polymer ages after it has been plastically deformed, the stored internal energy decreases with time. We think that the

relaxation of the stored energy is observed through the loss of orientation of the chains (decrease of *trans-trans* conformers (Figure 4.4)).

While at first glance it seems that no differences appear in the temperature-frequency position of the α-relaxation (Figures 4.1, 4.2), fitting revealed that the Vogel activation energy E_V is increased from 5.21 kJ/mol, after cold rolling, to 7.35 kJ/mol after subsequent ageing, implying that the molecular packing is more dense. In Chapter 3, the IV-transition was attributed to defect helices formed with deformation. With the information that the IV-transition still exists after ageing, we conclude that the polymer has not returned to a completely amorphous state, so there is no complete disappearance of the defect helices, which may be part of the fibrillar material. In a former study, Wool et al.[123] observed that complete craze healing in a-PS can happen at an ageing temperature of 70 °C. In our BDRS study, the ageing is studied at 50 °C, 20 K bellow the temperature at which complete healing has been observed. We conclude that small amounts of fibrilar material still exist in our case, since the ageing was applied at a relatively low temperature and for a short time.

4.5 Conclusions

Employing broadband dielectric relaxation spectroscopy, it is shown that the I(γ)- and II(γ')-relaxation processes merge after ageing at 50 °C for three hours. At the same time, the III-process is suppressed and the IV-process appears broader with a lower intensity. The main α-relaxation shows an increased Vogel activation energy. Fourier transform infrared spectroscopy confirms the decrease of the *trans-trans* population with ageing while, at the same time, the main-chain vibrations increase slightly.

We suggest that ageing after mechanical rejuvenation (cold rolling) is governed by structural reorganization back to the isotropic state through loss of orientation of the chains, which can be seen by the decrease in the *trans-trans* conformers. The suppression of the III-process and peak-intensity decrease of the IV-process confirms that the structures made upon cold rolling start to vanish and the sample returns to a more isotropic state with increased structural heterogeneity.

Chapter 5

Physical ageing of polystyrene: Does tacticity play a role?

Abstract: The ageing kinetics of amorphous atactic (a-PS), isotactic (i-PS) and syndiotactic (s-PS) polystyrene were studied by means of flash-differential scanning calorimetry (flash-DSC). The specimens were aged for up to two hours at six different ageing temperatures: the optimum ageing temperature, i.e. the temperature at which the enthalpy overshoot at the

This chapter is largely reproduced from: K. Grigoriadi, J.B.H.M. Westrik, G.G. Vogiatzis, L.C.A van Breemen, P.D. Anderson, M. Hütter. "Physical ageing of polystyrene: Does tacticity play a role?". To be submitted.

glass transition is maximal for given elapsed time, and five ageing temperatures ranging from 20 K to 80 K below the optimum ageing temperature. A logarithmic increase of the enthalpy overshoot with ageing time is observed for specimens at their optimum ageing temperatures. For temperatures significantly lower than the optimum, there is a range where the enthalpy overshoot is constant, but for higher temperatures (still below the optimum) also a logarithmic increase is observed. Moreover, the ageing kinetics appear to depend on tacticity, with s-PS and i-PS exhibiting the slowest and fastest ageing kinetics, respectively, while a-PS exhibiting ageing kinetics between these two extremes.

5.1 Introduction

Glasses are known to be far from their thermodynamic equilibrium and their structural relaxation towards equilibrium, via a sequence of molecular rearrangements, is known as physical ageing[8]. Physical ageing of polymeric glasses is known to affect the material properties, like the mechanical[13,47] or gas-transport properties,[58] posing limitations on their applications. A lot of studies have been conducted on the influence of physical ageing of glassy polymers on yielding[8,13,47,124,125], creep[43,46,84], volume relaxation[25,43,45,52,55,126], enthalpy changes[19,20,46,51,52], molecular-scale dynamics[34,60,127,128] and structural changes[31,82,83]. However, the connection between the molecular structure and the ageing kinetics has not yet been established.

Despite the fact that numerous techniques are employed to study the large number of properties affected by physical ageing in glassy polymers, only one of them can cool and heat the material rapidly enough to allow probing of the ageing kinetics by starting from a "true" rejuvenated amorphous state. This technique is flash-differential scanning calorimetry (flash-DSC) in which ultra-high heating and cooling rates (> 100.000 K/min) can be applied[129]. The majority of the ageing studies with flash-DSC involve measurements concerning a single material such as atactic polystyrene (a-

PS)[130–133], polycarbonate (PC)[131] and poly lactic-acid (PLA)[134]. Until now, there are only very few studies investigating the effect of tacticity on the ageing kinetics[135] of amorphous/glassy polymers. The main reason for the lack of studies is that syndiotactic and isotactic polymers, crystallize under normal cooling rates, resulting in a semi-crystalline material. For polystyrenes, there is another limiting factor next to the high crystallization rate[136] of s-PS, namely, its melting temperature, is very close to its degradation temperature, which makes the preparation of an amorphous sample in oxygen atmosphere impossible, because the material starts to degrade before the crystallinity is erased. The high crystallization rate can be tackled by the high cooling-rate that flash-DSC offers, and the complete melting of crystals before the material degrades has been taken care of by using a nitrogen atmosphere during the measurement.

In this work, we study the effect of tacticity on the ageing kinetics at high and low ageing temperatures for atactic, isotactic and syndiotactic polystyrene using flash-DSC in their amorphous/glassy state.

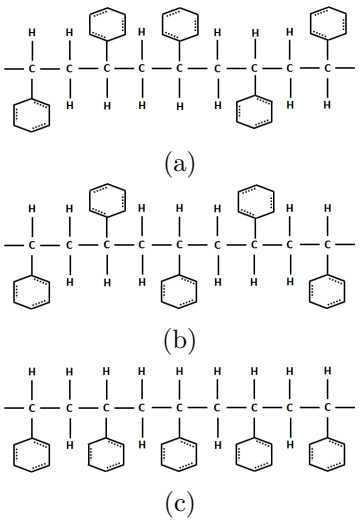

Figure 5.1: Stereochemistry of (a) atactic, (b) syndiotactic and (c) isotactic polystyrene.

5.2 Methodology

5.2.1 Materials

Atactic and syndiotactic PS (Figure 5.1) with syndio contents $\geq 90\%$ were bought in powder and pellet forms, respectively, from Polymer Source[137]. Their molecular weight is M_n = 412.000 g/mol with a polydispersity index PDI = 1.05 and M_n = 250.000 g/mol with a PDI = 3.5, respectively. Isotactic PS (Figure 5.1) with 90% isotactic content was bought in powder form from Scientific Polymer Products,[138] with a molecular weight of M_n = 400.000 g/mol and a PDI = 2.

5.2.2 Differential scanning calorimetry

Flash-differential scanning calorimetry: Experiments were carried out in a Mettler Toledo Flash-DSC 1 equipped with a Huber TC100 intra-cooler, under a constant flow of dry nitrogen using UFS1 sensors.

Differential-scanning calorimetry: Experiments were carried out in a Mettler-Toledo 823e/700 module with a Cryostat intra-cooler using a 50 μl aluminum pan under a constant flow of dry nitrogen.

5.2.3 Sample preparation

For the flash-DSC measurements, very small specimens of material of approximately 30 - 170 ng were cut and put onto the sensor with the use of an eyelash. For the conventional DSC, the powder-form samples were put in an aluminum pan with a mass between 5 mg and 10 mg.

Estimation of sample mass

In the case of the flash-DSC measurements, the sample mass cannot be measured with a conventional scale since the weight is too small (ng). For semicrystalline materials, the mass can be estimated as follows. A sample of known mass is cooled and heated in conventional DSC at 20 K/min and the specific melting enthalpy (Δh_m) is calculated by peak integration of the heating curve. Afterwards, a sample of unknown mass is cooled at 20

K/min and heated at 1000 K/s in the flash-DSC equipment. The melting enthalpy (ΔH_{m}) is calculated from the heating curve, and the mass of the flash-DSC sample can be determined by

$$m_{\mathrm{sc}} = \frac{\Delta H_{\mathrm{m}}}{\Delta h_{\mathrm{m}}}. \tag{5.1}$$

In the case of amorphous polymers, the sample mass can be estimated by using the method of Cebe et al.[139], employing the liquid heat capacity from flash-DSC (cooling rate 1000 K/s) and the specific heat-capacity from the ATHAS bank[140]. The sample mass m_{am} is determined by

$$m_{\mathrm{am}} = \frac{C_{p_{\mathrm{FDSC}}}}{c_{p_{\mathrm{DSC}}}}, \tag{5.2}$$

with, $C_{p_{\mathrm{FDSC}}}$ the heat capacity obtained from the flash-DSC experiments far above the glass transition temperature and $c_{p_{\mathrm{DSC}}}$ the specific liquid heat capacity taken from the ATHAS bank. The validity of the method is confirmed by applying both Equation 5.1 and Equation 5.2 to a semicrystalline sample. The error between the two mass-estimation methods is found to be about 5%.

Methods

In order to study the ageing kinetics of the selected materials, the temperature protocol shown in Figure 5.2 was used. The following steps can be identified: Step i: the sample was heated well above T_g (a-PS) or T_m (s-PS and i-PS) at a rejuvenation temperature T_{rej} (Table 5.1 and Figure 5.2) in order to erase its thermomechanical history (i.e. thermal rejuvenation). Step ii: the sample was rapidly quenched at a cooling rate of 1000 K/s to an end-quenching temperature T_q well below T_g, and subsequently heated rapidly (heating rate: 1000 K/s) above T_g to obtain the heating curve which serves as a reference state. Step iii: the sample is rapidly quenched (1000 K/s) and then heated (1000 K/s) to the chosen ageing temperature, T_a, and held at that temperature for a specific ageing time t_a. Step iv: the sample was quenched rapidly (1000K/s) at 25 °C for ageing temperatures higher than 25 °C and 0 °C for ageing temperatures below 25 °C to capture the aged state and heated rapidly (1000 K/s) above T_g (or T_m) to obtain the endothermic peak caused by ageing, and to thermally rejuvenate the sample for the next measurement. Step v: one more cycle of quenching and heating was performed to validate the rejuvenated state of the polymer (heating curve).

Table 5.1: Glass-transition temperature, T_g, and melting temperature, T_m, for a-PS, s-PS and i-PS, measured during heating with a heating rate of 1000 K/s, and rejuvenation, T_{rej}, and end-quenching temperatures, T_q. The end-quenching temperature is 25 °C for ageing temperatures higher than 25 °C and 0 °C for ageing temperatures below 25 °C.

sample	T_g (°C)	T_m (°C)	T_{rej} (°C)	T_q (°C)
a-PS	128	-	190	25 and 0
s-PS	124	270	310	25 and 0
i-PS	126	240	270	25 and 0

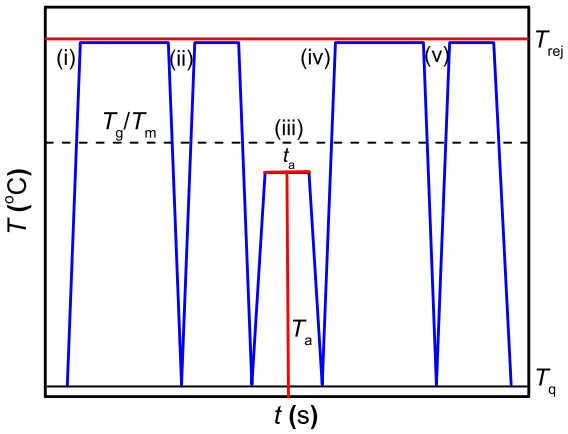

Figure 5.2: Schematic representation for the flash-DSC heating protocol: (i) Heating above T_g or T_m, (ii) reference-state heating-curve, (iii) isothermal ageing for ageing time t_a and at temperature T_a, (iv) aged-state heating-curve, and (v) reference-state heating-curve. The values of rejuvenation, T_{rej}, and end-quenching temperature, T_q, are provided in Table 5.1.

Analysis

The analysis of experimental data concerning the cooling-rate dependence of T_g and physical ageing can be analyzed in terms of enthalpy loss (ΔH_a) or the fictive temperature (T_f)[131]. Tool[141] defined T_f as a measure of the glass structure. The intersection of the extrapolated glass line and the extrapolated liquid line determines T_f. The T_f of an aged glass is related to the change in enthalpy with ageing[131],

$$\Delta H_a = \int_{T_{f_0}}^{T_f} \Delta C_p dT, \tag{5.3}$$

where ΔH_a is the enthalpy loss upon ageing, T_f the fictive temperature of the aged glass, T_{f_0} the fictive temperature of the unaged glass, and ΔC_p the step change in heat capacity. During physical ageing, T_{f_0} decreases to an equilibrium value, while ΔH_a increases from a zero value to the enthalpy equilibrium value[131]. We chose to analyze our data using the ΔH_a changes. Both types of analysis will yield identical conclusions/observations. The analysis procedure is described below.

Fitting a straight line to the liquid regime[131]: The calculation of the enthalpy overshoot of the aged specimen (i.e. the integral under the $C_p(T)$-curve) relies on drawing an unbiased liquid line, especially when a large overshoot is present. Thus, each heating scan was superposed with the

subsequent scan of a freshly quenched specimen. The liquid line was determined as the best linear fit of the $C_{\mathrm{p}}(T)$-curve at high temperatures, away from the enthalpy overshoot and the transition region. A consistent liquid line is crucial for calculating the integral under the $C_{\mathrm{p}}(T)$-curve. As shown in Figure 5.3, the enthalpy overshoot of the aged specimen is calculated in between the point where the $C_{\mathrm{p}}(T)$-curve departs from the linear liquid line till the point where it intersects again. This integral is considered positive. Then, we apply the same procedure to the rejuvenated sample and subtract its integral from that of the aged one.

Determination of excess enthalpy : The excess enthalpy was determined using the method of Petrie[142] in which the enthalpy loss ΔH_{a} upon ageing is calculated by the difference of the integrated $C_{\mathrm{p}}(T)$-curves of the aged and reference (rejuvenated) material (Figure 5.3),

$$\Delta H_{\mathrm{a}} = \int_{T_{\mathrm{a}}}^{T_{\mathrm{c}}} (C_{\mathrm{p}})_{\mathrm{aged}} dT - \int_{T_{\mathrm{a}}}^{T_{\mathrm{c}}} (C_{\mathrm{p}})_{\mathrm{ref}} dT. \tag{5.4}$$

Two measurements per sample are conducted for each ageing time and temperature.

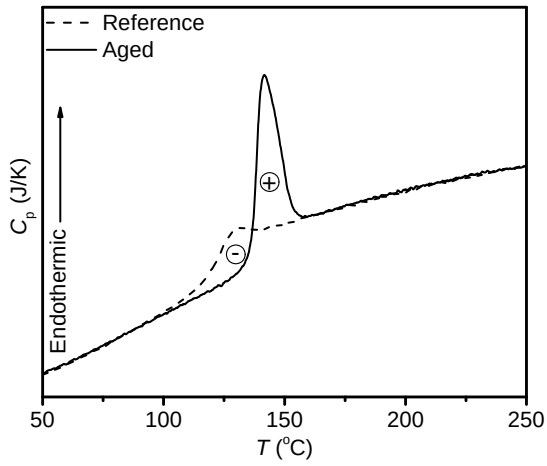

Figure 5.3: Representative curve for the calculation of the enthalpy loss ΔH_a upon ageing, according to the Petrie method[142].

Sensor corrections

Conditioning and correction was performed on the flash-DSC chip sensors before the sample is positioned on the sensor according to the manufacturers recommended protocol. No additional temperature corrections were applied, since the calibration by the manufacturer was found to have an error of about 0.6 - 0.7 K[143].

5.3 Results

In Figure 5.4, the flash-DSC heating-curves for atactic, syndiotactic and isotactic amorphous PS annealed at various ageing temperatures and ageing times are shown. It can be seen that the area of the endothermic peak as well as the temperature where the endothermic peak appears are increasing with the ageing time. Also, the cease of existence of a melting peak, as a result of the high cooling rate (1000 K/s) in case of semicrystalline polymers, validates that the samples are in an amorphous state (Figure 5.4).

We study the effect of ageing temperature T_{a} on the excess enthalpy ΔH_{tot} - ΔH_{rej} for an annealing time of ten minutes for atactic, syndiotactic and isotactic amorphous PS (Figure 5.5). Figure 5.5-a shows that for a-PS the excess enthlapy is increasing linearly with temperature where it reaches a maximum at around 102 °C ($\approx$ 26 K below the glass-transition temperature). After this temperature, the enthalpy overshoot decreases linearly. Similarly, the s-PS (Figure 5.5-b) excess enthalpy follows a linear increase with an optimum at $\approx$ 96 °C, ($\approx$ 28 K below T_{g}) and a decrease after this optimum as well. i-PS (Figure 5.5-c) has a similar behavior with an optimum enthalpy overshoot at $\approx$ 94 °C (32 K below T_{g}). Based on these results, we choose the temperature in which each polymer shows the largest overshoot as the optimum ageing temperature (T_{opt}), determined

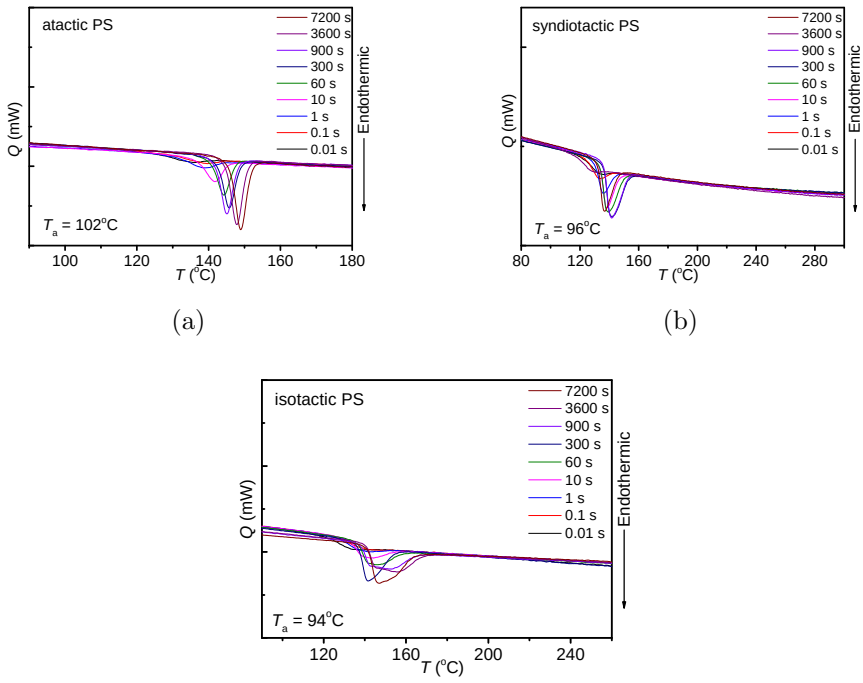

Figure 5.4: Heat flow Q versus temperature T for (a) a-PS, (b) s-PS and (c) i-PS, for various ageing times.

by fitting a polynomial of fifth order to the ΔH_{tot} - ΔH_{rej} versus T_{a} data (Figure 5.5). We perform measurements also at 20 K ($T_{\text{opt-20 K}}$), 30 K ($T_{\text{opt-30 K}}$), 40 K ($T_{\text{opt-40 K}}$), 60 K ($T_{\text{opt-60 K}}$) and 80 K ($T_{\text{opt-80 K}}$) below T_{opt} for all specimens.

In Figure 5.6, the excess enthalpy (ΔH_{tot} - ΔH_{rej}) as function of the

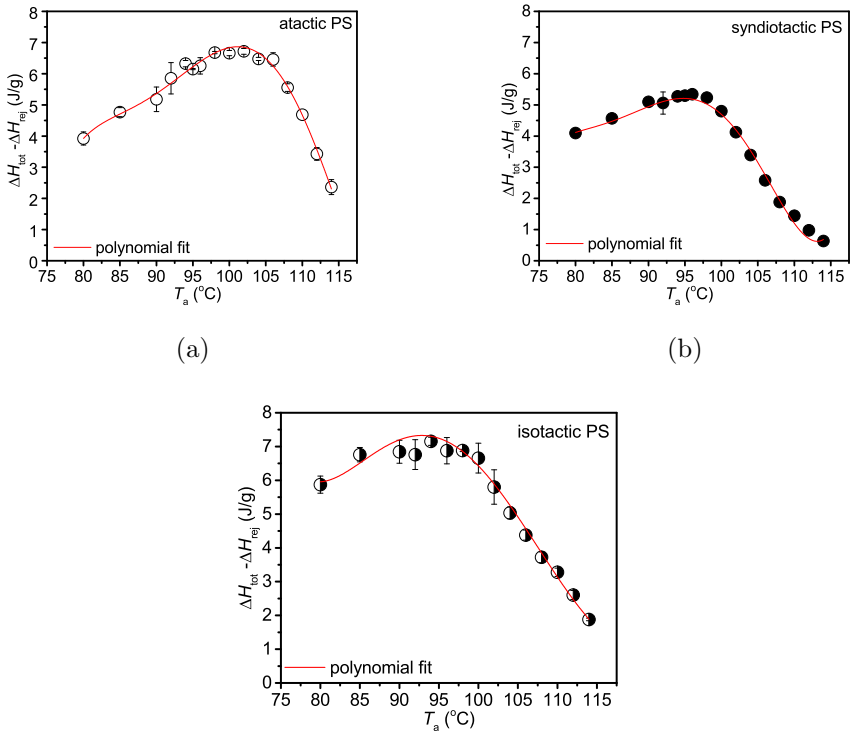

(a) (b)

(c)

Figure 5.5: Excess enthalpy, ΔH_{tot} - ΔH_{rej}, versus annealing temperature, T_{a}, for (a) a-PS, (b) s-PS and (c) i-PS. The ageing time is $t_{\mathrm{a}} = 10$ min. Lines represent the polynomial fits (see main text).

ageing time for the various ageing temperatures for atactic, syndiotactic and isotactic PS are shown. It can be seen that ΔH_{tot} - ΔH_{rej} follows a logarithmic increase with time for the optimum ageing temperatures. For very short ageing times ($\leq$ 0.1s), the ΔH_{tot} - ΔH_{rej} for the three PS speci-

mens is close to zero. For longer ageing times ($\geq$ 10s), the excess enthalpy shows a logarithmic increase for all specimens. At ageing temperatures below the optimum (Figure 6), it can be observed that the increase of ΔH_{tot} - ΔH_{rej} does not follow a logarithmic increase and is reduced compared to that for long ageing times. Similar to the observations for maximum ageing temperature for short ageing times, the enthalpy overshoot observed for the three PS specimens is close to zero.

Using time-temperature superposition, an activation energy can be determined. In Figure 5.7, the ΔH_{tot} - ΔH_{rej} curves are shifted horizontally along the logarithmic ageing-time axis, taking T_{opt} as a reference. The good superposition of lines allows to calculate the activation energy by plotting the logarithmic shift-factor (a_T) as a function of temperature and obtaining an Arrhenius plot for temperatures from $T_{\mathrm{opt\text{-}40\ K}}$ to $T_{\mathrm{opt\text{-}20\ K}}$. The activation energies E_{a} for a-PS, s-PS and i-PS calculated from the slope (E_{a}/R, where R is the gas constant) in Figure 5.8 are found to be (166.3 $\pm$ 4.0) kJ/mol for a-PS, (163.8 $\pm$ 6.0) kJ/mol for s-PS and (144.4 $\pm$ 9.7) kJ/mol for i-PS. Even if we take the lowest values for E_{a}/R for a-PS and s-PS, we cannot reach the highest value for i-PS. This indicates that despite the differences being subtle, they are by no means negligible.

The slope in the Arrhenius plot (Figure 5.8) for a-PS calculated in this work has a value of around 20 kK, while the slope calculated in the work of

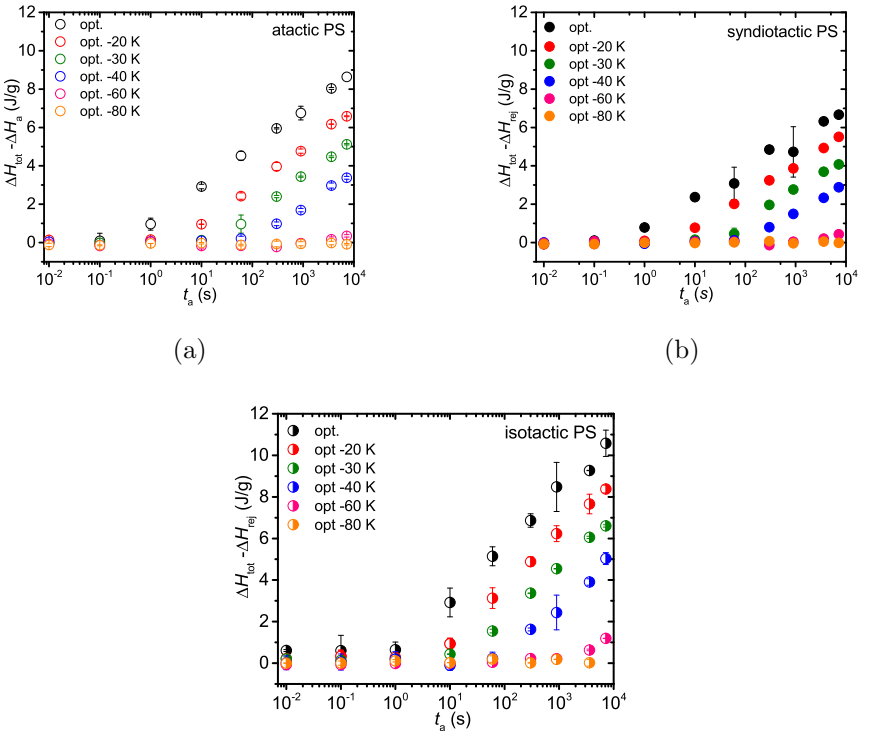

Figure 5.6: Excess enthalpy, ΔH_{tot} - ΔH_{rej}, versus ageing time, t_{a}, for (a) a-PS, (b) s-PS and (c) i-PS.

Koh et al.[143] has a value of 13 kK. Considering that in this work we used a limited temperature range for the construction of the Arrhenius plot in Figure 5.8 compared to the work of Koh et al.[143], errors may have been introduced due to the errors in the shift factors.

Furthermore, we quantify the ageing rate from the slope where ΔH_{tot} - ΔH_{rej} has a linear increase with respect to the logarithm of time,

$$R_{\mathrm{ag}} = \frac{d(\Delta H_{\mathrm{tot}} - \Delta H_{\mathrm{rej}})}{d(\ln t_{\mathrm{a}})}. \tag{5.5}$$

In Figure 5.9, the ageing rate, R_{ag}, is plotted as a function of the ageing temperature T_{a}. At $T_{\text{opt-80 K}}$, R_{ag} is close to zero, increases slightly with ageing temperature at $T_{\text{opt-60 K}}$, and has a large increase at $T_{\text{opt-40 K}}$. The ageing rates for i-PS, a-PS and s-PS are comparable for temperatures from $T_{\text{opt-80 K}}$ to $T_{\text{opt-40 K}}$. In addition, a-PS exhibits higher ageing rates than s-PS for temperatures above $T_{\text{opt-40 K}}$, where i-PS has the highest ageing rate of all specimens at the optimum T_{a}.

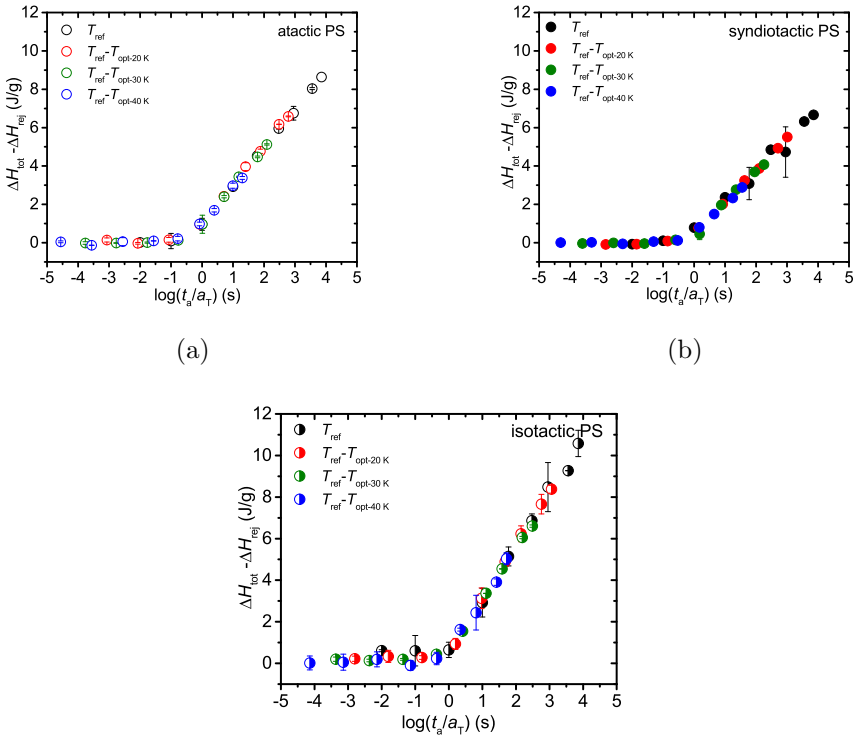

(a) (b)

(c)

Figure 5.7: Excess enthalpy obtained from time-temperature superposition using the optimum ageing temperature as the reference, $T_{\mathrm{ref}} = T_{\mathrm{opt}}$, for (a) a-PS, (b) s-PS and (c) i-PS.

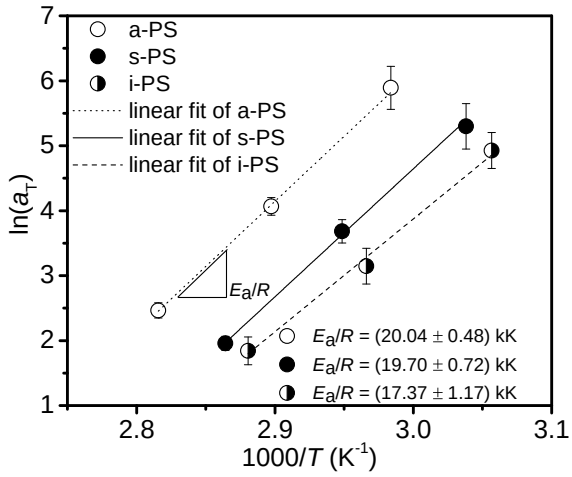

Figure 5.8: Arrhenius plot of the shift factor, a_T, for i-PS (half-filled circles), s-PS (filled circles) and a-PS (empty circles). The activation energy is represented by the slope of the lines.

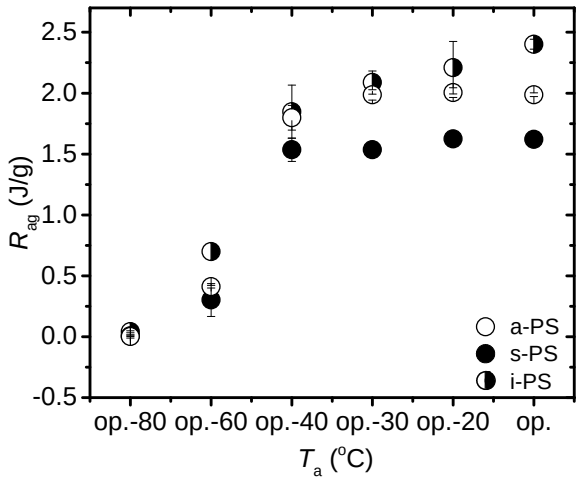

Figure 5.9: Ageing rate (R_{ag}) as a function of ageing temperature for i-PS (half-filled circles), s-PS (filled circles) and a-PS (empty circles).

5.4 Discussion

PS[19,144] as well as other glassy polymers such as PC[15,145] and PVC[146] have been reported to have logarithmic enthalpy-overshoot increase at high-temperature ageing. For ageing at the optimum ageing-temperature, the enthalpy overshoot increases logarithmically with time. For ageing temperatures below the optimum ageing-temperatures, ageing shows a non-logarithmic dependence on time. The farther the material is from its optimum ageing temperature, the longer it stays in an arrested state until it shows a logarithmic enthalpy-increase with time (Figure 5.6), similar to the enthalpy increase which has been reported for PC[145].

While all materials exhibit the same ageing mechanisms for all temperatures (logarithmic excess-enthalpy increase with T_{opt}, and delayed increase of the excess enthalpy with ageing at temperatures far below optimum), it is worth noting the effect of tacticity on the ageing rate. Specifically, a-PS and i-PS show a similar ageing-rate for temperatures from $T_{\text{opt-40 K}}$ to $T_{\text{opt-20 K}}$, while at the optimum ageing-temperature the fastest ageing-kinetics are observed for i-PS. s-PS shows the slowest ageing-kinetics between the three polymers, specifically for temperatures from $T_{\text{opt-40 K}}$ to T_{opt}.

We believe that the reason behind the difference of the rate at which

a-PS, s-PS and i-PS are ageing is related to the difference in chain flexibility of those polymers. Nakaoki et al.[147] studied, by solid state high resolution ^{13}C-NMR, the gauche content of amorphous atactic, syndiotactic and isotactic PS, finding 27.9%, 25.0% and 34.3%, respectively. Based on their results, they concluded that i-PS is more likely to have fewer trans sequences, which leads to a shorter random coil and to a smaller characteristic ratio (C_∞). This has been confirmed by small-angle neutron scattering (SANS) studies which have revealed that the characteristic ratio is $C_\infty^{\mathrm{s-PS}} > C_\infty^{\mathrm{a-PS}} > C_\infty^{\mathrm{i-PS}}$, that points out that the stiffest chain is the one of s-PS[148]. Specifically, the $C_\infty^{\mathrm{s-PS}}$ is 7.9 to 13 for increasing M_w from 214.000 g/mol to 380.000 g/mol[149]. The $C_\infty^{\mathrm{a-PS}}$ is 6.7 to 9.6 for increasing M_w from 325.000 to 500.000 g/mol, and the $C_\infty^{\mathrm{i-PS}}$ is 4.9 and 5 for M_w = 254.000 g/mol and 500.000 g/mol, respectively[149]. Syndiotactic sequences make the polymer chain rigid[150] and slow down the reorganization of the chains, which consequently leads to slower ageing kinetics, as it has been shown in our measurements (Figure 5.9). Tensile creep measurements on polyimide Kapton-H and cellulose acetate butyrate ester have also suggested that the ageing kinetics are slower for the polymer with more rigidity of the main chain[151].

One could think that ageing and crystallization underlie the same physics. This work, however, shows that they are not correlated directly.

Ageing kinetics are governed by the chain flexibility, while crystallization kinetics are strongly dependent on the stereoregularity of the polymer. For the case of PS, s-PS crystallizes about hundred times faster than i-PS[152]; the main reason for that is the conformation of the C-C backbone in these polymers. The backbone of s-PS has a planar zig-zag conformation, while the backbone of i-PS has a 3/1 helical conformation[152]. Moreover, i-PS has higher work of chain folding than s-PS[152]. Conclusively, the backbone conformation of s-PS together with the low work of chain folding are related to its high-crystallization rate contrary to i-PS. In contrast, in our work, we show that s-PS ages slower than i-PS due to its chain being more rigid[148].

5.5 Conclusions

The effect of tacticity on the ageing kinetics of glassy amorphous PS was investigated by flash-DSC. Our results show that the tacticity does have an effect on the physical ageing kinetics, with syndiotactic and isotactic PS showing the two extremes, slow and fast ageing kinetics, respectively, while atactic PS shows ageing kinetics between these two extremes.

The enthalpy overshoot of all PS's follows a logarithmic increase with ageing time at the optimum ageing temperatures. For temperatures far below its optimum, there is a range, different for each specimen, where the enthalpy overshoot is constant, whereas at higher temperatures (but still below the optimum temperature), it also shows a logarithmic increase. In addition, the activation energy for i-PS is found to be the lowest, while the activation energies of a-PS and s-PS have the same values within the experimental error.

Finally, this study shows that ageing and crystallization do not underlie the same physics; the governing factor for ageing kinetics is the chain flexibility, while the crystallization kinetics are governed by the stereoregularity of the polymer.

Chapter 6

Connections with modeling and simulations

In this chapter, the most intriguing experimental findings are being connected with results from computational studies.

Observations:

- For the thermally rejuvenated a-PS, only the α- and γ-relaxations can be observed (*Chapter 2*).
- After short-term ageing, the α- and γ-relaxations are observed. Moreover, a β*-relaxation close to the α-relaxation appears (*Chapter 2*).

- After long-term ageing, the α-, β*-, and γ-relaxations are observed. Here, the β*- and γ-relaxations frequency peaks move to lower temperatures with ageing, i.e. relaxation times increase (*Chapter 2*).

- After cold rolling, next to the known α- and γ- relaxations, three new relaxations are observed, II(γ')-, III- and IV-relaxations, with the IV-relaxation showing a peculiar behavior: in its low-temperature part, it has a high positive activation energy. At around 70 °C, the relaxation seems to shift towards low frequencies together with a strong decrease in its intensity, similar to a melting transition (*Chapter 3*).

The position of the α-relaxation does not change, either it is not affected by ageing, or part of the history of the sample has been erased upon heating before reaching the α-relaxation frequency-temperature regime. The β*- and γ-relaxations seem to be affected by ageing. The relaxation times increase with ageing time.

Problem statement:

1. Why are secondary relaxations (β* and γ) affected by ageing?

2. What is the origin of the peculiar IV-transition?

Current consensus:

- The segmental α-relaxation process freezes at the glass-transition

temperature. In general, the α-process is a collective process, which shows strong non-Arrhenius like behavior[153].

- The faster, sub-T_g, processes (β* and γ) are more "Arrhenius-like"and less collective in the glassy regime.

- The β-process appears for a-PS around a frequency of 110 Hz at T = 47 °C and has an activation energy of about 130 kJ/mol[41]. However, by varying the annealing conditions, the barrier will also vary between 90 and 170 kJ/mol.[154] At high frequencies, the peak of the β-process merges with the α-relaxation peak. It is believed that the β-process of PS originates from a local oscillation mode of the backbone chain[41].

- The γ-process has been reported to have and activation energy of 34-38 kJ/mol[155], 35 kJ/mol for rejuvenated a-PS[34] and 43 kJ/mol for PS aged for ten months at 20 °C[34]. Other studies reported energy barrier heights in the range of 21-29 kJ/mol[156]. It has been associated with the phenyl-ring flip[157]. Recent studies show that there is no phenyl-ring association[71,158].

Insight obtained by molecular simulations:

In a dense polymeric material (either melt or glass), the backbone dihedral angles cannot rotate freely, without hindering other chains as well. Rapold et al.[159] estimated the mean energy for a phenyl-ring flip at 116 kJ/mol, by

employing an energy minimization method to a fully atomistic PS model. The actual distribution of barrier heights was found to be very broad, in the range of 0.96-1115 kJ/mol (for the cases in which the energetic barrier was positive). The frequency distribution for the ring motion covers many orders of magnitude and small reorientation of phenyl rings dominate the dynamics below T_g. The fraction of phenyl rings flipping was found to be less than 3%.

The Molecular Dynamics (MD) simulations of Lyulin et al.[160] below T_g showed, for both phenyl rings and main chain, translational and rotational motions. Their characteristic times correspond quite well to those reported for β- and γ-relaxations, respectively. The dynamics of phenyl rings and main chain had very similar characteristic times and were considered correlated due to excluded-volume interactions. Later, Vorselaars et al.[157] conducted 25ns-MD runs to study the phenyl-ring flip in polystyrene, which is thought to be the molecular origin of the γ-relaxation. These authors observed that upon cooling the system towards the glass transition the motion of the phenyl ring becomes more heterogeneous. They speculated that this results from a distribution of local energy barriers in combination with slower transitions between states separated by these local energy barriers. The fraction of flipping observed during a 25-ns-run was 2%.

Boulougouris and Theodorou[158] studied the sub-glass segmental relax-

ation in a-PS up to times on the order of 10^{-5} s. They probed the molecular mechanism of the γ- and δ-processes and identified the δ-process with rotation of a single phenyl group around its stem. The most probable candidate of the γ-process motion was the vibration of the phenyl stem and ring. This motion was immensely random. There were phenyl rings whose stems have decorrelated up to 42% at 10^{-5} s, whereas others remained practically frozen over the simulation time. These authors speculated that the low mobility occurs in regions with a high degree of local tacticity along the a-PS chain.

Lyulin et al.[161] studied by MD simulations the effect of uniaxial extension on the mobility of the monomers of glassy a-PS and PC. Below the yield point, no significant changes were observed in the mobility of the monomers, while above the yield point they observed parallel diffusion accelerated by more than one order of magnitude. In addition, finite element simulations show that for plastic deformation at 30% strain, 45% of the applied work is converted into stored energy[162].

Final hypothesis:

1. Physical ageing induces densification of the material which comes as a result of the local neighborhood being driven to close-packed conformations. This is confirmed by the FTIR measurements which indicate an increase of the *trans-trans* conformations. For this densification

to take place, phenyl rings should flip, as expected by molecular simulations also. Finally, the densified regions (of local tacticity) are less mobile, resulting in relaxation processes with higher activation energies (as measured by BDRS).

2. Cold rolling leads to an increased molecular mobility and high internal energy storage, which is confirmed by molecular simulations and BDRS.

Chapter 7

Conclusions and recommendations

This thesis is an endeavour to understand the molecular origins of physical ageing and rejuvenation, both mechanical and thermal. Broadband dielectric relaxation spectroscopy (BDRS) in combination with attenuation reflectance Fourier transform infrared spectroscopy (ATR-FTIR) is used to examine the effect of thermal rejuvenation and low-temperature ageing on atactic polystyrene (a-PS) (Chapter 2), the molecular differences between thermal and mechanical rejuvenation of a-PS (Chapter 3) and the mechanism of ageing after cold rolling (Chapter 4). With flash differential scanning calorimetry (flash-DSC), the effect of tacticity on the ageing kinetics of glassy polystyrene was assessed (Chapter 5). This thesis provides molecular insight into the understanding of physical ageing of glassy

polymers.

7.1 Conclusions

Effect of low-temperature physical ageing on the dynamic transitions of atactic polystyrene in the glassy state (Chapter 2)

- Ageing deep in the glassy state affects the β*- and γ-processes.
- Ageing increases the *trans-trans* conformers, characteristic of states that are energetically more favorable[85].

Transient dynamics of cold-rolled and subsequently thermally rejuvenated atactic-polystyrene (Chapter 3)

- Microscopically, mechanical and thermal rejuvenation are of very different nature. While in thermal rejuvenation the main characteristic is homogeneity and low molecular mobility, the mechanical rejuvenation is governed by heterogeneity and high mobility.
- A mechanically rejuvenated specimen resembles microscopically a specimen that consists of three phases: (i) an isotropic-amorphous phase, (ii) an oriented-amorphous phase and (iii) a nano-crystalline phase.

This three-phase structure could explain the origin of the ductility of mechanically rejuvenated specimens.

Dynamics of cold-rolled and subsequently aged atactic-polystyrene (Chapter 4)

- Ageing after plastic deformation at temperatures around 50 °C, below the glass-transition temperature, is manifested by molecular reorganization towards a more isotropic and dense structure.

Physical ageing of polystyrene: Does tacticity play a role? (Chapter 5)

- Physical-ageing kinetics depend on stereoregularity. Syndiotactic and isotatic PS exhibit slowest and fastest ageing kinetics, respectively, while atactic PS displays ageing kinetics between these two extremes.

7.2 Recommendations

The work in this thesis provides answers to questions about the molecular mechanisms responsible for low-temperature ageing, and thermal and mechanical rejuvenation of glassy polystyrene, based on experimental observations. The findings of this work will stimulate discussions and encourage further research, as explained in the following.

Low temperature ageing vs. high temperature ageing. Low-temperature ageing is recently getting attention as a molecularly different mechanism [78,163] (Chapter 1). An investigation of FTIR and Raman spectroscopy on the role of molecular conformations at long-term low-temperature aged specimens compared to high-temperature aged specimens can shed more light on the molecular differences between these two different ageing mechanisms.

An interesting finding of both this study and the work of Wypych et al.[34] is the increase of intensity and activation energy of the γ-relaxation with low-temperature ageing (Chapter 2). A focused investigation on the effect of ageing on the γ-relaxation with combined BDRS and neutron scattering experiments will give more direct information about the actual structural feautures on the molecular scale during ageing.

Thermal vs. mechanical rejuvenation. The findings presented in Chapter 3 could only be unveiled by following a unique experimental protocol: Fast-BDRS measurements in a continuous temperature and frequency mode were the key to study the transient state of cold-rolled a-PS by BDRS. Still, there are limitations on the rate at which the equipment can cool and heat. Specifically for cases with fast ageing-kinetics, the sample ages during the scan, therefore one needs higher-speed measurements, to avoid interference of the measurement scan with the on-going ageing. The design and creation of an ultrafast BDRS is therefore necessary.

Certainly, the molecular mechanism of mechanical rejuvenation unveiled in Chapter 2 has to be investigated further. Special attention should be given to confirm the existence of the nano-crystalline regions. Recommended experimental methods are X-ray scattering (e.g. WAXS) and electron microscopy (e.g. TEM and SEM). Moreover, in our study ATR-FTIR was used to detect the nano-crystalline regions; the drawback of this technique is that it can measure up to 3 μm in thickness. Transmision FTIR is recommended to be applied in the conformationally sensitive region 400 cm^{-1} to 600 cm^{-1} in order to measure the whole material.

Ageing after mechanical deformation. Ageing after mechanical deformation (Chapter 4) shows different molecular mechanisms in comparison to ageing after thermal rejuvenation (Chapter 2). It is suggested that this be followed by a sequential BDRS experiment at different temperatures and times, which will provide more information on the molecular mechanism after plastic deformation.

Another intriguing finding that was not discussed in this thesis was the effect of different treatments on the molecular vibrations of a-PS (Figure 7.1) as measured by transmission FTIR. Consider for example the behavior of the methylene main-chain vibration (Figure 7.1(b)-(c)) and the aromatic CH-stretching vibration (Figure 7.1(d)-(e)) with thermal rejuvenation and subsequent ageing (Figure 7.1(b)-(d)) and cold rolling and subsequent

ageing (Figure 7.1(c)-(e)). While the main-chain and ring vibrations show an increase of glass-transition temperature with ageing after thermal rejuvenation, the results for the cold-rolled and aged samples are intriguing: the main chain after ageing has a lower glass-transition temperature, while the ring vibration does not show a transition in this temperature range. A thorough experimental analysis of the FTIR spectra of a polymer with different treatments can reveal important information on the molecular mechanisms that each treatment creates. The findings can be used as input to atomistic simulations and quantum mechanical calculations, and consequently deliver the molecular picture for each treatment.

Computational deformational experiments can shed light on the mechanism of mechanical rejuvenation. It is recommended to pay special attention to the changes of free volume and molecular changes during and after deformation.

Physical ageing kinetics and their relation to the molecular structure. In view of the findings of Chapter 5, which reveal that physical ageing kinetics are tacticity dependent, it is proposed to investigate the relation between the chain stiffness and the physical-ageing kinetics by flash-DSC. The chain stiffness can be estimated by low-frequency Raman spectroscopy (disordered-longitudinal acoustic mode, D-LAM). In low-frequency Raman spectroscopy studies[164], it has been seen that the D-LAM frequency incre-

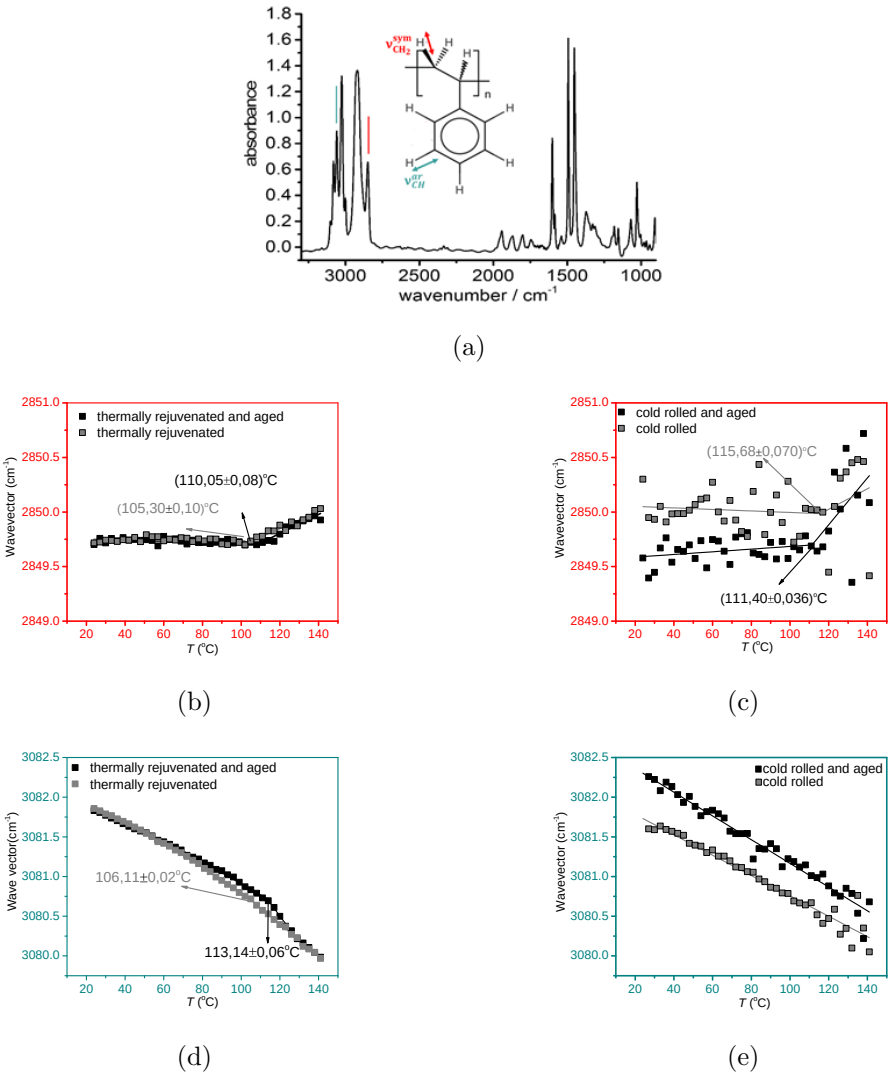

Figure 7.1: (a) IR spectrum of atactic polystyrene. Red arrow: symmetric main chain vibration; green arrow: ring vibration. (b, c) Main chain symmetric vibrations and (d, e) ring vibrations for thermally rejuvenated, cold-rolled and subsequently aged samples.

ases in the order of i-PS < a-PS < s-PS, meaning that the chain stiffness increases in the same order. Also, small-angle neutron scattering (SANS) experiments have shown that the characteristic ratio increases also in the order $C_{\infty}^{\mathrm{i-PS}} < C_{\infty}^{\mathrm{a-PS}} < C_{\infty}^{\mathrm{s-PS}}$ [149]; it can be observed that chain stiffness, characteristic ratio and ageing kinetics have an inverse relation: the increase of chain stiffness and characteristic ratio is related to the slowing-down of the ageing kinetics, as it has been shown in our flash-DSC study (i-PS > a-PS > s-PS). This relation is proposed to be investigated for other polymers with different stereoregularity, e.g atactic, isotactic and syndiotactic PMMA. Moreover, it is suggested to study the effect of the introduction of side groups to a polymeric chain on chain stiffness, characteristic ratio and physical ageing. The side groups should be of different size and complexity, and be introduced to polymers with a relatively simple molecular structure, such as PS and PC.

Flash-DSC is certainly a technique that can provide useful information in very short time. Still, the placement of a specimen on a sensor is time consuming. Moreover, the costly sensor is susceptible to damage because of the force that the user applies for placing the sample on the sensor. It is proposed to manufacture a robot that can automatically cut and place the sample on the sensor, which is cost and time efficient. Furthermore, cutting and placing the sample on the sensor directly after its treatment

has the advantage of rapid measurement after a treatment (e.g. mechanical treatment of the sample) when fast reorganization processes can occur (ageing). Here, measurements need to be done at the first heating run, which is possible with the use of a contact medium such as silone oil[129].

Universality confirmation. The universal character of the experimental protocols followed needs to be confirmed. It is suggested that other glassy polymers, such as polycarbonate (PC), a polymer that has been studied macroscopically (e.g. yield stress) and microscopically (e.g. conformational changes) extensively in our and other groups[165–172], are analyzed in a similar fashion. Poly(methyl methacrylate) (PMMA) is also an interesting candidate, since its molecular structure is of increased complexity as compared to PS and PC. From an industrial point of view, PMMA can be considered an alternative to PC when properties such as e.g. transparency and UV tolerance are more important than for e.g. the high impact-strength and chemical resistance of PC[173] with a big advantage: It does not contain the bisphenol-A monomer, which is harmful for the human health[174–177].

Undeniably, focused studies should be carried out on "green" polymers which have been recently studied more intensely, such as poly-lactic acid (PLA) and chitosan. PLA is a polymer well researched for its biodegradable life cycle[178] and its medical applications[179,180]. Chitosan, a polymer produced from biodegradable resources, has drawn a lot of attention, in

view of antimicrobial packaging applications[178,181,182] and drug delivery systems[178].

References

[1] J. D. Lytle. Polymeric optics. In *Book Handbook of optics, Devices, Measurements and Properties, Second Edition*, page 34. Optical Scociety of America, United States of America, 1995.

[2] A. J. Hill and M. R. Tant. The structure and properties of glassy polymers, an overview. In *Book Structure and properties of glassy polymers, First Edition*, pages 1–20. ACS Symposium Series Vol. 710, American Chemical Society: Washington, DC., 1998.

[3] J. R. Klaehn, C. J. Orme, E. S. Peterson, F. F. Stewart, and J. M. Urban-Klaehn. High temperature gas separations using high performance polymers. In *Book Inorganic Polymeric and Composite Membranes Structure, Function and Other Correlations, First Edition*, pages 295–307. Elsevier B. V: Amsterdam, 2011.

[4] A. Gleadall. Mechanical properties of biodegradable polymers for medical applications. In *Book Modelling Degradation of Bioresorbable Polymeric Medical Devices*, pages 163–199. Elsevier B. V.: London, 2015.

[5] Perry baromedical, hyperbaric therapy systems. http://perrybaromedical.mivamerchant.net/hyperbaric-systems-monoplace.html, 2013. [Online; accessed 8-February-2019].

[6] V. Doushkina. Advantages of polymer and hybrid glass-polymer optics. https://www.photonics.com/Articles/a41974, 2010. [Online; accessed 8-February-2019].

[7] M. Sepe. Materials: The mystery of physical aging: Part 1. https://www.ptonline.com/columns/the-mystery-of-physical-aging-part-1, 2014. [Online; accessed 8-February-2019].

[8] L. C. E. Struik. Physical aging in plastics and other glassy materials. *Polym. Eng. Sci.*, 17(3):165–173, 1977.

[9] J.-H. Guo, R. E. Robertson, and G. L. Amidon. Influence of physical aging on mechanical properties of polymer free films: the prediction of long-term aging effects on the water permeability and dissolution rate of polymer film-coated tablets. *Pharm. Res.*, 8(12):1500–1504, 1991.

[10] G. W. Ehrenstein and S. Pongratz. *Resistance and stability of polymers*. Carl Hanser Verlag, Munich, 2013.

[11] J. M. G. Cowie and R. Ferguson. Physical ageing of poly (met-

hyl methacrylate) from enthalpy relaxation measurements. *Polymer*, 34(10):2135–2141, 1993.

[12] G. B. McKenna and A. J. Kovacs. Physical aging of poly (methyl methacrylate) in the nonlinear range: Torque and normal force measurements. *Polym. Eng. Sci.*, 24(14):1138–1141, 1984.

[13] H. G. H. Van Melick, L. E. Govaert, B. Raas, W. J. Nauta, and H. E. H. Meijer. Kinetics of ageing and re-embrittlement of mechanically rejuvenated polystyrene. *Polymer*, 44(4):1171–1179, 2003.

[14] A. L. Volynskii, A. V. Efimov, and N. F. Bakeev. Structural aspects of physical aging of polymer glasses. *Polym. Sci. Ser. C*, 49(4):301–320, 2007.

[15] J. M. Hutchinson, S. Smith, B. Horne, and G. M. Gourlay. Physical aging of polycarbonate: Enthalpy relaxation, creep response, and yielding behavior. *Macromolecules*, 32(15):5046–5061, 1999.

[16] I. M. Hodge and A. R. Berens. Effects of annealing and prior history on enthalpy relaxation in glassy polymers. 2. Mathematical modeling. *Macromolecules*, 15(3):762–770, 1982.

[17] L. C. E. Struik. *Physical aging in amorphous polymers and other materials.* Elsevier, Amsterdam, 1980.

[18] Y. Nanzai, A. Miwa, and S. Z. Cui. Mechanical and thermal analysis of aging in strained polymethyl methacrylate. *JSME Int. J. A-Solid M.*, 42(4):479–484, 1999.

[19] D. J. Hourston, M. Song, A. Hammiche, H. M. Pollock, and M. Reading. Modulated differential scanning calorimetry: 2. Studies of physical ageing in polystyrene. *Polymer*, 37(2):243–247, 1996.

[20] A. R. Berens and I. M. Hodge. Effects of annealing and prior history on enthalpy relaxation in glassy polymers. 1. Experimental study on poly (vinyl chloride). *Macromolecules*, 15(3):756–761, 1982.

[21] O. A. Hasan and M. C. Boyce. Energy storage during inelastic deformation of glassy polymers. *Polymer*, 34(24):5085–5092, 1993.

[22] O. B. Salamatina, G. W. H. Höhne, S. N. Rudnev, and E. F. Oleinik. Work, heat and stored energy in compressive plastic deformation of glassy polymers. *Thermochim. Acta*, 247(1):1–18, 1994.

[23] L. J. Broutman and R. S. Patil. Cold rolling of polymers. 1 influence of rolling on properties of amorphous polymer. *Polym. Eng. Sci.*, 11(2):165–173, 1971.

[24] D. Cangialosi, Michael Wübbenhorst, J. Groenewold, E. Mendes, H. Schut, A. Van Veen, and S. J. Picken. Physical aging of poly-

carbonate far below the glass transition temperature: evidence for the diffusion mechanism. *Phys. Rev. B*, 70(22):224213, 2004.

[25] B. Wang, W. Gong, W. H. Liu, Z. F. Wang, N. Qi, X. W. Li, M. J. Liu, and S. J. Li. Influence of physical aging and side group on the free volume of epoxy resins probed by positron. *Polymer*, 44(14):4047–4052, 2003.

[26] B. Bending, K. Christison, J. Ricci, and M. D. Ediger. Measurement of segmental mobility during constant strain rate deformation of a poly (methyl methacrylate) glass. *Macromolecules*, 47(2):800–806, 2014.

[27] H.-N. Lee, K. Paeng, S. F. Swallen, and M. D. Ediger. Direct measurement of molecular mobility in actively deformed polymer glasses. *Science*, 323(5911):231–234, 2009.

[28] J. Kalfus, A. Detwiler, and A. J. Lesser. Probing segmental dynamics of polymer glasses during tensile deformation with dielectric spectroscopy. *Macromolecules*, 45(11):4839–4847, 2012.

[29] Y. G. Chung and D. J. Lacks. How deformation enhances mobility in a polymer glass. *Macromolecules*, 45(10):4416–4421, 2012.

[30] Y. G. Chung and D. J. Lacks. Sheared polymer glass and the question of mechanical rejuvenation. *J. Chem. Phys.*, 136(12):124907, 2012.

[31] J. Lu, Y. Wang, and D. Shen. Infrared spectroscopic and modulated differential scanning calorimetric study of physical aging in bisphenol-A polycarbonate. *Polym. J.*, 32(7):610–615, 2000.

[32] G. J. Salomons, M. A. Singh, T. Bardouille, W. A. Foran, and M. S. Capel. Small-angle x-ray scattering study of craze formation and dynamics in thermoplastics. *Macromolecules*, 32(4):1264–1270, 1999.

[33] A. L. Volynskii and N. F. Bakeev. Healing of interfacial surfaces in polymer systems. *Polym. Sci. Ser. A*, 51(10):1096, 2009.

[34] A. Wypych, E. Duval, G. Boiteux, J. Ulanski, L. David, G. Seytre, A. Mermet, I. Stevenson, M. Kozanecki, and L. Okrasa. Physical aging of atactic polystyrene as seen by dielectric relaxational and low-frequency vibrational raman spectroscopies. *J. Non-Cryst. Solids*, 351(33-36):2593–2598, 2005.

[35] S. J. Lupaşcu, V. Picken and M. Wübbenhorst. Dynamics of T2G2 helices in atactic and syndiotactic polystyrene: New evidence from dielectric spectroscopy and ftir. *Macromolecules*, 39(15):5152–5158, 2006.

[36] B. Natesan, H. Xu, Seyhan I. B., and P. Cebe. Molecular relaxation of isotactic polystyrene: Real-time dielectric spectroscopy and x-ray scattering studies. *J. Polym. Sci. B Pol. Phys.*, 42(5):777–789, 2004.

[37] J. Y. Cavaille, C. Jourdan, J. Perez, L. Monnerie, and G. P. Johari. Time-temperature superposition and dynamic mechanical behavior of atactic polystyrene. *J. Polym. Sci. B Pol. Phys.*, 25(6):1235–1251, 1987.

[38] K. C. M. Nair, S. Thomas, and G. Groeninckx. Thermal and dynamic mechanical analysis of polystyrene composites reinforced with short sisal fibres. *Compos. Sci. Technol.*, 61(16):2519–2529, 2001.

[39] S. Yu and P. Hing. Dynamic mechanical properties of polystyrene-aluminum nitride composite. *J. Appl. Polym. Sci.*, 78(7):1348–1353, 2000.

[40] P. Atorngitjawat, R. J. Klein, and J. Runt. Dynamics of sulfonated polystyrene copolymers using broadband dielectric spectroscopy. *Macromolecules*, 39(5):1815–1820, 2006.

[41] O. Yano and Y. Wada. Dynamic mechanical and dielectric relaxations of polystyrene below the glass temperature. *J. Polym. Sci., Part B: Polym. Phys.*, 9(4):669–686, 1971.

[42] K. Schmieder and K. Wolf. Mechanische relaxationserscheinungen en hochpolymeren. *Kolloid-Z*, 134:149–189, 1953.

[43] M. D. Shelby and G. L. Wilkes. The effect of molecular orientation on the physical ageing of amorphous polymers-dilatometric and mechanical creep behaviour. *Polymer*, 39(26):6767–6779, 1998.

[44] G. B. McKenna, Y. Leterrier, and C. R. Schultheisz. The evolution of material properties during physical aging. *Polym. Eng. Sci.*, 35(5):403–410, 1995.

[45] R. Pixa, V. Le Dû, and C. Wippler. Dilatometric study of deformation induced volume increase and recovery in rigid pvc. *Colloid Polym. Sci.*, 266(10):913–920, 1988.

[46] L. B. Liu, A. F. Yee, and D. W. Gidley. Effect of cyclic stress on enthalpy relaxation in polycarbonate. *J. Polym. Sci. B Pol. Phys.*, 30(3):221–230, 1992.

[47] C. Ho Huu and T. Vu-Khanh. Effects of physical aging on yielding kinetics of polycarbonate. *Theor. Appl. Fract. Mech.*, 40(1):75–83, 2003.

[48] J. M. Hutchinson. Physical aging of polymers. *Prog. Polym. Sci.*, 20(4):703–760, 1995.

[49] S. M. Kuo and E. M. Woo. Sub-Tg molecular relaxation and enthalpy relaxation behavior in amorphous glassy poly (ether imide). *J. Polym. Res.*, 4(4):213–219, 1997.

[50] E. Flikkema, G. Alberda van Ekenstein, and G. Ten Brinke. Temperature modulated calorimetry of glassy polymers and polymer blends. *Macromolecules*, 31(3):892–898, 1998.

[51] Y. Kubota, K. Fukao, and Y. Saruyama. Heat flows on the heating process after aging of glassy poly (methyl methacrylate) measured by temperature modulated differential scanning calorimeter. *Thermochim. Acta*, 431(1-2):149–154, 2005.

[52] S. K. Burgess, C. R. Mubarak, R. M. Kriegel, and W. J. Koros. Physical aging in amorphous poly (ethylene furanoate): Enthalpic recovery, density, and oxygen transport considerations. *J. Polym. Sci. B Pol. Phys.*, 53(6):389–399, 2015.

[53] K. M. Nairn, G. P. Simon, A. J. Hill, and R. L. Walters. Differential scanning calorimetry as a measurement technique for physical ageing in polycarbonate. In *Materials Forum (Australia)*, volume 16, pages 167–172, 1992.

[54] K. D. Dorkenoo and P. H. Pfromm. Experimental evidence and the-

oretical analysis of physical aging in thin and thick amorphous glassy polymer films. *J. Polym. Sci. B Pol. Phys.*, 37(16):2239–2251, 1999.

[55] Y. Huang, X. Wang, and D. R. Paul. Physical aging of thin glassy polymer films: Free volume interpretation. *J. Membrane Sci.*, 277(1-2):219–229, 2006.

[56] B. W. Rowe, B. D. Freeman, and D. R. Paul. Physical aging of ultrathin glassy polymer films tracked by gas permeability. *Polymer*, 50(23):5565–5575, 2009.

[57] B. W. Rowe, B .D. Freeman, and D. R. Paul. Influence of previous history on physical aging in thin glassy polymer films as gas separation membranes. *Polymer*, 51(16):3784–3792, 2010.

[58] C. M. Laot, E. Marand, B. Schmittmann, and R. K. P. Zia. Effects of cooling rate and physical aging on the gas transport properties in polycarbonate. *Macromolecules*, 36(23):8673–8684, 2003.

[59] C. Zhou, T. S. Chung, R. Wang, and S. H. Goh. A governing equation for physical aging of thick and thin fluoropolyimide films. *J. Appl. Polym. Sci.*, 92(3):1758–1764, 2004.

[60] R. Casalini and C. M. Roland. Aging of the secondary relaxation

to probe structural relaxation in the glassy state. *Phys. Rev. Lett.*, 102(3):035701, 2009.

[61] G. Power, J. K. Vij, and G. P. Johari. Kinetics of spontaneous change in the localized motions of d-sorbitol glass. *J. Chem. Phys.*, 124(7):074509, 2006.

[62] O. van den Berg, W. G. F. Sengers, W. F. Jager, S. J. Picken, and M. Wübbenhorst. Dielectric and fluorescent probes to investigate glass transition, melt, and crystallization in polyolefins. *Macromolecules*, 37(7):2460–2470, 2004.

[63] M. Wübbenhorst and J. van Turnhout. Analysis of complex dielectric spectra. I. One-dimensional derivative techniques and three-dimensional modelling. *J. Non-Cryst. Solids*, 305(1-3):40–49, 2002.

[64] J. van Turnhout and M. Wübbenhorst. Analysis of complex dielectric spectra. II. Evaluation of the activation energy landscape by differential sampling. *J. Non-Cryst. Solids*, 305(1-3):50–58, 2002.

[65] S. N. Magonov, D. Shen, and R. Qian. Fourier transform infra-red spectroscopy of atactic polystyrene in the glass transition region. *Macromol. Chem. Phys.*, 190(10):2563–2570, 1989.

[66] W. G. F. Sengers, O. Van den Berg, M. Wübbenhorst, A. D. Gotsis,

and S. J. Picken. Dielectric spectroscopy using dielectric probes: a new approach to study glass transition dynamics in immiscible apolar polymer blends. *Polymer*, 46(16):6064–6074, 2005.

[67] S. J. Lupaşcu, V. Picken and M. Wübbenhorst. Cooperative and non-cooperative dynamics in ultra-thin films of polystyrene studied by dielectric spectroscopy and capacitive dilatometry. *J. Non-Cryst. Solids*, 352(52-54):5594–5600, 2006.

[68] M. Theodorou, B. Jasse, and L. Monnerie. Fourier-transform infrared investigation of conformational changes occurring at the yield point in uniaxially drawn atactic polystyrene. *J. Polym. Sci. B Pol. Phys.*, 23(3):445–450, 1985.

[69] J. B. Enns, R. F. Boyer, H. Ishida, and J. L. Koenig. Fourier transform infrared spectroscopic study of transitions above tg in atactic polystyrene. *Polym. Engin. Sci.*, 19(10):756–759, 1979.

[70] W. Yanxiang and S. Deyan. Supermolecular structure of gelation of atactic polystyrene/carbon disulphide solutions. *Polym. Bull.*, 39(5):633–638, 1997.

[71] S. Arrese-Igor, A. Arbe, B. Frick, and J. Colmenero. Glassy dynamics

of polystyrene by quasielastic neutron scattering. *Macromolecules*, 44(8):3161–3168, 2011.

[72] S. Etienne and D. Laurent. Long-term physical ageing of amorphous polymers. *Philos. Mag.*, 87(3-5):417–424, 2007.

[73] E. Schlosser and A. Schönhals. Dielectric relaxation during physical ageing. *Polymer*, 32(12):2135–2140, 1991.

[74] A. Alegria, L. Goitiandia, I. Telleria, and J. Colmenero. α-relaxation in the glass-transition range of amorphous polymers. 2. Influence of physical aging on the dielectric relaxation. *Macromolecules*, 30(13):3881–3887, 1997.

[75] P. Lunkenheimer, R. Wehn, U. Schneider, and A. Loidl. Glassy aging dynamics. *Phys. Rev. Lett.*, 95(5):055702, 2005.

[76] J. Zhao and G. B. McKenna. Temperature divergence of the dynamics of a poly (vinyl acetate) glass: Dielectric vs. mechanical behaviors. *J. Chem. Phys.*, 136(15):154901, 2012.

[77] I. M. Hodge and G. S. Huvard. Effects of annealing and prior history on enthalpy relaxation in glassy polymers. 3. Experimental and modeling studies of polystyrene. *Macromolecules*, 16(3):371–375, 1983.

[78] N. G. Perez-De Eulate and D. Cangialosi. The very long-term physical aging of glassy polymers. *Phys. Chem. Chem. Phys.*, 20(18):12356–12361, 2018.

[79] D. P. B. Aji and G. P. Johari. Kinetic-freezing and unfreezing of local-region fluctuations in a glass structure observed by heat capacity hysteresis. *J. Chem. Phys.*, 142(21):214501, 2015.

[80] L. C. E. Struik. *Physical aging in amorphous polymers and other materials*. PhD thesis, TU Delft, 1977.

[81] L. C. A. Van Breemen, T. A. P. Engels, E. T. J. Klompen, Dirk J. A. Senden, and L. E. Govaert. Rate-and temperature-dependent strain softening in solid polymers. *J. Polym. Sci. B Pol. Phys.*, 50(24):1757–1771, 2012.

[82] N. Heymans. Ftir investigation of structural modification of polycarbonate during thermodynamical treatments. *Polymer*, 38(14):3435–3440, 1997.

[83] P. Pan, B. Zhu, T. Dong, K. Yazawa, T. Shimizu, M. Tansho, and Y. Inoue. Conformational and microstructural characteristics of poly (l-lactide) during glass transition and physical aging. *J. Chem. Phys.*, 129(18):184902, 2008.

[84] V. A. Soloukhin, J. C. M. Brokken-Zijp, O. L. J. van Asselen, and G. de With. Physical aging of polycarbonate: Elastic modulus, hardness, creep, endothermic peak, molecular weight distribution, and infrared data. *Macromolecules*, 36(20):7585–7597, 2003.

[85] B. C. Laskowski, D. Y. Yoon, D. McLean, and R. L. Jaffe. Chain conformations of polycarbonate from ab initio calculations. *Macromolecules*, 21(6):1629–1633, 1988.

[86] Y. Wang, D. Shen, and R. Qian. Subglass-transition-temperature annealing of poly (ethylene terephthalate) studied by ftir. *J. Polym. Sci. B Pol. Phys.*, 36(5):783–788, 1998.

[87] J .L. Koenig and M. K. Antoon. Thermally induced conformational changes in poly (vinyl chloride). *J. Polym. Sci. B Pol. Phys.*, 15(8):1379–1395, 1977.

[88] P. G. Debenedetti and F. H. Stillinger. Supercooled liquids and the glass transition. *Nature*, 410(6825):259–267, 2001.

[89] L. C. E Struik. Physical aging in amorphous glassy polymers. *Ann. N. Y. Acad. Sci.*, 279(1):78–85, 1976.

[90] D. Cangialosi, M. Wübbenhorst, H. Schut, A. Van Veen, and S. J. Picken. Amorphous-amorphous transition in glassy polymers sub-

jected to cold rolling studied by means of positron annihilation lifetime spectroscopy. *J. Chem. Phys.*, 122(6):064702, 2005.

[91] D. L. Malandro and D. J. Lacks. Relationships of shear-induced changes in the potential energy landscape to the mechanical properties of ductile glasses. *J. Chem. Phys.*, 110(9):4593–4601, 1999.

[92] G. Gagnon, J. Patton, and D. J. Lacks. Energy landscape view of fracture and avalanches in disordered materials. *Phys. Rev. E.*, 64(5):051508, 2001.

[93] S. S. Jang and W. H. Jo. Analysis of the mechanical behavior of poly (trimethylene terephthalate) in an amorphous state under uniaxial extension–compression condition through atomistic modeling. *J. Chem. Phys.*, 110(15):7524–7532, 1999.

[94] G. B. McKenna. Mechanical rejuvenation in polymer glasses: fact or fallacy? *J. Phys. Condens. Matter*, 15(11):S737–S763, 2003.

[95] A. V. Lyulin, D. Hudzinskyy, E. Janiaud, and A. Chateauminois. Competition of time and spatial scales in polymer glassy dynamics: Rejuvenation and confinement effects. *J. Non-Cryst. Solids*, 357(2):567–574, 2011.

[96] H. N. Lee and M. D. Ediger. Mechanical rejuvenation in poly (methyl

methacrylate) glasses? molecular mobility after deformation. *Macromolecules*, 43(13):5863–5873, 2010.

[97] M. M. Santore, R. S. Duran, and G. B. McKenna. Volume recovery in epoxy glasses subjected to torsional deformations: the question of rejuvenation. *Polymer*, 32(13):2377–2381, 1991.

[98] S. L. Simon, J. W. Sobieski, and D. J. Plazek. Volume and enthalpy recovery of polystyrene. *Polymer*, 42(6):2555–2567, 2001.

[99] G. B. McKenna, Y. Leterrier, and C. R. Schultheisz. The evolution of material properties during physical aging. *Polym. Eng. Sci.*, 35(5):403–410, 1995.

[100] P. A. O'connell and G. B. McKenna. Large deformation response of polycarbonate: Time-temperature, time-aging time, and time-strain superposition. *Polym. Eng. Sci.*, 37(9):1485–1495, 1997.

[101] R. Pérez-Aparicio, D. Cottinet, C. Crauste-Thibierge, L. Vanel, P. Sotta, J. Y. Delannoy, D. R. Long, and S. Ciliberto. Dielectric spectroscopy of a stretched polymer glass: heterogeneous dynamics and plasticity. *Macromolecules*, 49(10):3889–3898, 2016.

[102] V. Lupaşcu, S. J. Picken, and M. Wübbenhorst. Dynamics of t2g2 helices in atactic and syndiotactic polystyrene: New evidence from

dielectric spectroscopy and ftir. *Macromolecules*, 39(15):5152–5158, 2006.

[103] Jr. H. W. Starkweather. Simple and complex relaxations. *Macromolecules*, 14(5):1277–1281, 1981.

[104] P. Papadopoulos, W. Kossack, and F. Kremer. Intra-and intermolecular dynamics in glass-forming liquids. *Soft Matter*, 9(5):1600–1603, 2013.

[105] D. Olmos, E. V. Martin, and J. Gonzalez-Benito. New molecular-scale information on polystyrene dynamics in ps and ps–batio3 composites from ftir spectroscopy. *Phys. Chem. Chem. Phys.*, 9(44):24339–24349, 2014.

[106] G. Guerra, P. Musto, F. E. Karasz, and W. J. MacKnight. Fourier transform infrared spectroscopy of the polymorphic forms of syndiotactic polystyrene. *Makromol. Chem.: Macromol. Chem. Phys.*, 191(9):2111–2119, 1990.

[107] Y. S. Sun, E. M Woo, M. C. Wu, and R.-M. Ho. Waxd and ftir spectroscopy studies on phase behavior of syndiotactic polystyrene/1, 1, 2, 2-tetrachloroethane complexes. *Polymer*, 44(18):5293–5302, 2003.

[108] F. J. Torres, B. Civalleri, A. Meyer, P. Musto, A. R. Albunia, P. Rizzo, and G. Guerra. Normal vibrational analysis of the syndiotactic polystyrene s(2/1)2 helix. *J. Phys. Chem. B*, 113(15):5059–5071, 2009.

[109] K. Tashiro, Y. Ueno, A. Yoshioka, and M. Kobayashi. Molecular mechanism of solvent-induced crystallization of syndiotactic polystyrene glass. 1. time-resolved measurements of infrared/raman spectra and x-ray diffraction. *Macromolecules*, 34(2):310–315, 2001.

[110] M. Kobayashi, T. Nakaoki, and N. Ishihara. Polymorphic structures and molecular vibrations of syndiotactic polystyrene. *Macromolecules*, 22(11):4377–4382, 1989.

[111] A. Grassi, P. Longo, and G. Guerra. Solid-state high-resolution 13c nmr spectra of syndiotactic polystyrene. *Makromol. Chem. Rapid Comm.*, 10(12):687–690, 1989.

[112] M. A. Gomez and A. E. Tonelli. Carbon-13 nuclear magnetic resonance study of chain conformation in the solid polymorphs of syndiotactic polystyrene. *Macromolecules*, 23(13):3385–3386, 1990.

[113] Jr. H. W. Starkweather. Noncooperative relaxations. *Macromolecules*, 21(6):1798–1802, 1988.

[114] J. C. M. Li. Behavior and properties of shear bands. *Polym. Eng. Sci.*, 24(10):750–760, 1984.

[115] H. E. H Meijer and L. E. Govaert. Multi-scale analysis of mechanical properties of amorphous polymer systems. *Macromol. Chem. Physi.*, 204(2):274–288, 2003.

[116] H. E. H Meijer and L. E. Govaert. Mechanical performance of polymer systems: The relation between structure and properties. *Progr. Polym. Sci.*, 30(8-9):915–938, 2005.

[117] C. de Rosa and F. Auriemma. Influence of crystal defects and structural disorder on the physical and mechanical properties of polymeric materials. In *Crystals and Crystallinity in Polymers: Diffraction Analysis of Ordered and Disordered Crystals, First Edition*, pages 369–463. John Wiley and Sons: New Jersey, 2013.

[118] E. F. Oleinik, S. N. Rudnev, O. B. Salamatina, M. A. Mazo, I. A. Strelnikov, and M. I. Koteljansky. Energy accumulation and mechanism of plastic deformation in organic glassy polymers. In D. Hubbard, editor, *Plastic Deformation*, page 45. Nova Science Publishers: New York, 2016.

[119] S-S. Chang. Stored energy in poly (vinyl chloride) from pelletizing process. *J. Chem. Thermodyn.*, 9(2):189–197, 1977.

[120] L. L. Berger and B. B. Sauer. Enhanced segmental mobility at polymer surfaces: thermally stimulated current studies of crazed films. *Macromolecules*, 24(8):2096–2099, 1991.

[121] A. C-M Yang and E. J. Kramer. Craze fibril structure and coalescence by low-angle electron diffraction. *J. Polym. Sci. B Pol. Phys.*, 23(7):1353–1367, 1985.

[122] M. Dionisio and Mano J. F. *In Handbook of Thermal Analysis and Calorimetry Vol. 5: Recent Advances, Techniques and Applications.* Elsevier, Amsterdam the Netherlands, 2008.

[123] R. P. Wool and K. M. O'Connor. Craze healing in polymer glasses. *Polym. Eng. Sci.*, 21(14):970–977, 1981.

[124] C. G. Sell and G. B. McKenna. Influence of physical ageing on the yield response of model dgeba/poly (propylene oxide) epoxy glasses. *Polymer*, 33(10):2103–2113, 1992.

[125] T. S. Chow. Stress-strain behaviour of physically ageing polymers. *Polymer*, 34(3):541–545, 1993.

[126] D. Cangialosi, H. Schut, A. van Veen, and S. J. Picken. Positron annihilation lifetime spectroscopy for measuring free volume during physical aging of polycarbonate. *Macromolecules*, 36(1):142–147, 2003.

[127] P. Lunkenheimer, R. Wehn, and A. Loidl. Dielectric spectroscopy on aging glasses. *J. Non-Cryst. Solids*, 352(42-49):4941–4945, 2006.

[128] R. Wehn, P. Lunkenheimer, and A. Loidl. Broadband dielectric spectroscopy and aging of glass formers. *J. Non-Cryst. Solids*, 353(41-43):3862–3870, 2007.

[129] J. E. K. Schawe and S. Pogatscher. Material characterization by fast scanninc calorimetry: practice and applications. In J. Schick and D. Mathod, editors, *Fast Scanning Calorimetry*, pages 1–80. Springer International Publishing, 2016.

[130] Y. P. Koh, S. Gao, and S. L. Simon. Structural recovery of a single polystyrene thin film using flash dsc at low aging temperatures. *Polymer*, 96:182–187, 2016.

[131] S. L. Simon and Y. P. Koh. The glass transition and structural recovery using flash-dsc. In J. Schick and D. Mathod, editors, *Fast Scanning Calorimetry*, pages 433–459. Springer International Publishing, 2016.

[132] Y. P. Koh, L. Grassia, and S. L. Simon. Structural recovery of a single polystyrene thin film using nanocalorimetry to extend the aging time and temperature range. *Thermochim. Acta*, 603:135–141, 2015.

[133] Y. P. Koh and S. L. Simon. Structural relaxation of stacked ultrathin polystyrene films. *J. Polym. Sci. Part B: Polym. Phys.*, 46(24):2741–2753, 2008.

[134] X. Monnier, A. Saiter, and E. Dargent. Physical aging in pla through standard dsc and fast scanning calorimetry investigations. *Thermochim. Acta*, 648:13–22, 2017.

[135] S. Doulut, C. Bacharan, P. Demont, A. Bernes, and C. Lacabanne. Physical aging and tacticity effects on the α-relaxation mode of amorphous polymers by thermally stimulated techniques. *J. Non-Cryst. Solids*, 235:645–651, 1998.

[136] A. J. Pasztor Jr, B. G. Landes, and P. J. Karjala. Thermal properties of syndiotactic polystyrene. *Thermochim. Acta*, 177:187–195, 1991.

[137] Polymer source, inc. https://www.polymersource.ca/, 2019. [Online; accessed 8-February-2019].

[138] Scientific polymer products, inc. https://scientificpolymer.com/, 2019. [Online; accessed 8-February-2019].

[139] P. P. Cebe, B. P. Kaplan, D. L. Wurm, A. E. Zhuravlev, and C. Schick. Using flash-dsc for determining the liquid state heat capacity of silk fibroin. *Thermochim. Acta*, 615:8–14, 2015.

[140] M. Pyda. Polystyrene (ps) heat capacity, enthalpy, entropy, gibbs energy: Datasheet. In *The Advanced Thermal Analysis System (ATHAS) Databank – Polymer Thermodynamics*. Springer Materials, 2014.

[141] A. Q. Tool. Effect of heat-treatment on the density and constitution of high-silica glasses of the borosilicate type. *J. Am. Ceram. Soc.*, 31(7):177–186, 1948.

[142] S. E. B. Petrie. Thermal behavior of annealed organic glasses. *J. Polym. Sci. Part A-2: Polym. Phys.*, 10(7):1255–1272, 1972.

[143] Y. P. Koh and S. L. Simon. Enthalpy recovery of ultrathin polystyrene film using flash-dsc. *Polymer*, 143:40–45, 2018.

[144] R-J Roe and G.-M. Millman. Physical aging in polystyrene: Comparison of the changes in creep behavior with the enthalpy relaxation. *Polym. Eng. Sci.*, 23(6):318–322, 1983.

[145] C. H. Ho and T. Vu-Khanh. Effects of time and temperature on

physical aging of polycarbonate. *Theor. Appl. Fract. Mec.*, 39(2):107–116, 2003.

[146] A. J. Pappin, J. M. Hutchinson, and M. D. Ingram. Enthalpy relaxation in polymer glasses: evaluation and interpretation of the tool-narayanaswamy parameter x for poly (vinyl chloride). *Macromolecules*, 25(3):1084–1089, 1992.

[147] T. Nakaoki and M. Kobayashi. Local conformation of glassy polystyrenes with different stereoregularity. *J. Mol. Struct.*, 655(3):343–349, 2003.

[148] T. Takebe, K. Yamasaki, K. Funaki, and M. Malanga. Properties of syndiotactic polystyrene. In J. Schellenberg, editor, *Syndiotactic Polystyrene: Synthesis, Characterization, Processing, and Applications*, pages 295–307. John Wiley & Sons, Inc. Hoboken, NJ, USA, 2009.

[149] M. Kobayashi, S. Hanafusa, T. Yoshioka, and S. Koizumi. Molecular form and stereoregularity of polystyrenes in glassy state. *Kobunshi Ronbunshu*, 53:575–581, 1996.

[150] E. M. Woo and L. Chang. Tacticity in vinyl polymers. pages 1–22. Wiley Online Library, 4th Edition, 2002.

[151] G. Levita and L. C. E. Struik. Physical ageing in rigid chain polymers. *Polymer*, 24(8):1071–1074, 1983.

[152] K. Yamasaki, N. Tomotsu, and M. Malanga. Characterization, properies and applications of syndiotactic polystyrene. In J. Scheirs and D. Priddy, editors, *Modern styrenic polymers: polystyrenes and styrenic copolymers*, pages 389–409. Wiley, 2003.

[153] P. G. Debenedetti. Metastable liquids: Concepts and principles. Princeton University Press, New Jersey, 1996.

[154] S. Vyazovkin and I. Dranca. A dsc study of α-and β-relaxations in a ps-clay system. *J. Phys. Chem. B*, 108(32):11981–11987, 2004.

[155] S. N. Goyanes. Dynamic mechanical behavior of atactic and high-impact polystyrene. *J. Appl. Polym. Sci.*, 75(7):865–873, 2000.

[156] S. Reich and A. Eisenberg. Theoretical approach to the assignment of molecular mechanisms for cryogenic loss peaks in polymers. *J. Polym. Sci. A-2: Polym. Phys.*, 10(7):1397–1400, 1972.

[157] B. Vorselaars, A. V. Lyulin, and M. A. J. Michels. Development of heterogeneity near the glass transition: Phenyl-ring-flip motions in polystyrene. *Macromolecules*, 40(16):6001–6011, 2007.

[158] G. C. Boulougouris and D. N. Theodorou. Probing subglass relaxation in polymers via a geometric representation of probabilities, observables, and relaxation modes for discrete stochastic systems. *J. Chem. Phys.*, 130(4):044905, 2009.

[159] R. F. Rapold, U. W. Suter, and D. N. Theodorou. Static atomistic modelling of the structure and ring dynamics of bulk amorphous polystyrene. *Macromol. Theory Simul.*, 3(1):19–43, 1994.

[160] A. V. Lyulin, N. K. Balabaev, and M. A. J. Michels. Correlated segmental dynamics in amorphous atactic polystyrene: A molecular dynamics simulation study. *Macromolecules*, 35(25):9595–9604, 2002.

[161] A. V. Lyulin, B. Vorselaars, M. A. Mazo, N. K. Balabaev, and M. A. J. Michels. Strain softening and hardening of amorphous polymers: Atomistic simulation of bulk mechanics and local dynamics. *EPL (Europhysics Letters)*, 71(4):618–624, 2005.

[162] R. Xiao, G. Ghazaryan, T. A. Tervoort, and T. D. Nguyen. Modeling energy storage and structural evolution during finite viscoplastic deformation of glassy polymers. *Phys. Rev. E*, 95(6):063001, 2017.

[163] D. P. B. Aji and G. P. Johari. Kinetic-freezing and unfreezing of

local-region fluctuations in a glass structure observed by heat capacity hysteresis. *J. Chem. Phys.*, 142(21):214501, 2015.

[164] T. Kobayashi, M. Nakaoki and N. Ishihara. Molecular conformation in glasses and gels of syndiotactic and isotactic polystyrenes. *Macromolecules*, 23(1):78–83, 1990.

[165] L. E. Govaert, T. A. P. Engels, E. T. J. Klompen, G. W. M. Peters, and H. E. H. Meijer. Processing-induced properties in glassy polymers: development of the yield stress in PC. *Int. Polym. Proc.*, 20(2):170–177, 2005.

[166] E. T. J. Klompen, T. A. P. Engels, L. C. A. Van Breemen, P. J. G. Schreurs, L. E. Govaert, and H. E. H. Meijer. Quantitative prediction of long-term failure of polycarbonate. *Macromolecules*, 38(16):7009–7017, 2005.

[167] L. C. A. Van Breemen, L. E. Govaert, and H. E. H. Meijer. Scratching polycarbonate: A quantitative model. *Wear*, 274:238–247, 2012.

[168] J. Bartos, J. Müller, and J. H. Wendorff. Physical ageing of isotropic and anisotropic polycarbonate. *Polymer*, 31(9):1678–1684, 1990.

[169] T. Ricco and T. L. Smith. Rejuvenation and physical ageing of

a polycarbonate film subjected to finite tensile strains. *Polymer*, 26(13):1979–1984, 1985.

[170] J. M. Pérez, J. L. Vilas, J. M. Laza, S. Arnáiz, F. Mijangos, E. Bilbao, M. Rodríguez, and L. M. León. Effect of reprocessing and accelerated ageing on thermal and mechanical polycarbonate properties. *J. Mater. Proces. Tech.*, 210(5):727–733, 2010.

[171] C. Bauwens-Crowet and J. C. Bauwens. Rejuvenation and annealing effects on the loss curve of polycarbonate: 2. Cooling and ageing dependence. *Polymer*, 31(4):646–650, 1990.

[172] N. Heymans and S. van Rossum. FTIR investigation of structural modifications during low-temperature ageing of polycarbonate. *J. Mater. Sci.*, 37(20):4273–4277, 2002.

[173] Acrylic VS polycarbonate. https://www.hydrosight.com/acrylic-vs-polycarbonate-a-quantitative-and-qualitative-comparison/. [Online; accessed 12-March-2019].

[174] C. Erler and J. Novak. Bisphenol A exposure: human risk and health policy. *J. Pediatr. Nurs.*, 25(5):400–407, 2010.

[175] T. Groff. Bisphenol A: invisible pollution. *Curr. Opin. Pediatr.*, 22(4):524–529, 2010.

[176] L. N. Vandenberg and G. S. Prins. Clarity in the face of confusion: new studies tip the scales on bisphenol A (BPA). *Andrology*, 4(4):561, 2016.

[177] M. Murata and J.-H. Kang. Bisphenol A (BPA) and cell signaling pathways. *Biotechnol. Adv.*, 36(1):311–327, 2018.

[178] G. Z. Papageorgiou. Thinking green: Sustainable polymers from renewable resources. *Polymers*, 10(9):1–5, 2018.

[179] D. Li, G. Guo, R. Fan, J. Liang, X. Deng, F. Luo, and Z. Qian. PLA/F68/dexamethasone implants prepared by hot-melt extrusion for controlled release of anti-inflammatory drug to implantable medical devices: I. Preparation, characterization and hydrolytic degradation study. *Int. J. Pharm.*, 441(1-2):365–372, 2013.

[180] K. Hamad, M. Kaseem, H. W. Yang, F. Deri, and Y. G. Ko. Properties and medical applications of polylactic acid: A review. *Express Polym. Lett.*, 9(5):435–455, 2015.

[181] K. Grigoriadi, A. Giannakas, A. K. Ladavos, and N. M. Barkoula. Interplay between processing and performance in chitosan-based clay nanocomposite films. *Polym. Bull.*, 72(5):1145–1161, 2015.

[182] A. Giannakas, K. Grigoriadi, A. Leontiou, N. M. Barkoula, and A. La-

davos. Preparation, characterization, mechanical and barrier properties investigation of chitosan–clay nanocomposites. *Carbohyd. Polym.*, 108(8):103–111, 2014.

Curriculum vitae

Kalouda Grigoriadi

born on 15th of October, 1987 in Corfu, Greece

2019	**Doctor of Philosophy** Department of Mechanical Engineering, Eindhoven University of Technology, The Netherlands Thesis entitled "Molecular Origin of Physical Ageing and Rejuvenation in Glassy Polystyrene"
2014	**Master of Science in Chemistry and Technology of Materials** University of Ioannina, Greece Thesis entitled "Mechanical, thermal and thermo-mechanical study of novel biodegradable hybrid nanocomposites produced from renewable resources"
2010	**Dipl. Eng., Materials Science and Engineering** Department of Materials Science and Engineering, University of Ioannina, Greece

List of publications

This thesis has resulted in the following publications:

- K. Grigoriadi, T. Putzeys, M. Wübbenhorst, L.C.A van Breemen, P.D. Anderson and M. Hütter, Effect of low-temperature physical ageing on the dynamic transitions of atactic polystyrene in the glassy state, submitted to *J. Pol. Sci. Part B: Pol. Phys.*, **2019**.

- K. Grigoriadi, M. Wübbenhorst, L.C.A van Breemen, P.D. Anderson and M. Hütter, Transient dynamics of cold-rolled and subsequently thermally rejuvenated atactic-polystyrene using broadband dielectric spectroscopy, submitted to *Macromolecules*, **2019**.

- K. Grigoriadi, M. Wübbenhorst, L.C.A van Breemen, P.D. Anderson and M. Hütter, Dynamics of cold-rolled and subsequently aged atactic polystyrene. *To be submitted.*

- K. Grigoriadi, J.B.H.M. Westrik, G.G. Vogiatzis, L.C.A van Breemen, P.D. Anderson and M. Hütter, Physical ageing of polystyrene: Does tacticity play a role? *To be submitted.*

- K. Grigoriadi, M. Wübbenhorst, L.C.A van Breemen, P.D. Anderson and M. Hütter, Thermal vs. mechanical rejuvenation of a-PS: molecular dynamics reveal different microscopic scenarios. *Proceeding of the ACS Spring 2019 National Meeting & Expo*, Orlando-Florida, March 31 – April 4, 2019.

Additionally, the author contributed to papers outside the scope of this thesis:

- N. Jonkers, K. Grigoriadi, L.C.A van Breemen, P.D. Anderson and M. Hütter, Extracting intrinsic mechanical properties of glassy polymers from micro-indentation experiments in combination with finite element simulations. *To be submitted.*